IDENTIFYING SOILS WITH POTENTIAL OF EXPANDING SULFATE MINERAL FORMATION USING ELECTROMAGNETIC INDUCTION

A Thesis

by

MIRANDA L. FOX

Submitted to the Office of Graduate Studies of
Texas A&M University
in partial fulfillment of the requirements for the degree of

MASTER OF SCIENCE

August 2004

Major Subject: Soil Science

IDENTIFYING SOILS WITH POTENTIAL OF EXPANDING SULFATE MINERAL FORMATION USING ELECTROMAGNETIC INDUCTION

A Thesis

by

MIRANDA L. FOX

Submitted to the Office of Graduate Studies of
Texas A&M University
in partial fulfillment of the requirements for the degree of

MASTER OF SCIENCE

Approved as to style and content by:

C.T. Hallmark (Chair of Committee)	S. E. Feagley (Member)
S.W. Searcy (Member)	C.L.S. Morgan (Member)
M.A. Hussey (Head of Department)	

August 2004

Major Subject: Soil Science

ABSTRACT

Identifying Soils With Potential of Expanding Sulfate Mineral Formation Using Electromagnetic Induction. (August 2004)

Miranda L. Fox, B.S., Kansas State University

Chair of Advisory Committee: Dr. C.T. Hallmark

Sulfate-bearing soils are a problem in highway construction as they combine with materials used for lime stabilization to form minerals, particularly ettringite, that expand and induce heave in the stabilized soil. This research involves quantifying sulfate in soils that may be potentially used in highway construction using electromagnetic induction. The objectives are to: 1) document electrical conductivity (EC) variability within selected sites that contain sulfate-bearing materials, and 2) determine if electromagnetic induction has potential for locating hazardous levels of sulfate-bearing materials.

The 0.43 ha study area is located in the Blackland Prairies and is a Vertisol known to contain gypsum at the time of site selection. Apparent EC using a model EM38 electromagnetic induction instrument was measured at 200 locations in July and November 2003, using a sampling grid with 5-m spacings. Representative rows and columns were selected from the map of apparent electrical conductivity, and soil cores taken to a depth of 1.5 m at 29 points. Soil samples were obtained by dividing cores into depth increments of 0 to 25 cm, 25 to 75 cm, and 75 to 150 cm. Laboratory analyses were run for each sample and included moisture content, EC and soluble cations and anions of the saturated

paste extract, and percent gypsum. Elevation measurements were made to determine if changes in elevation related to EC measurements.

Apparent EC proved to be more successful at detecting soluble salts during the dry sampling period (July) when the effect of soil moisture content was less. For July data, EC and gypsum were significantly correlated in the deepest samples (r^2 = 0.51 and 0.15, respectively) to apparent EC. Further, soluble sulfate was significantly correlated to apparent EC (r^2 = 0.30) at a depth of 25 to 75 cm. Results suggest that the EM38 can be used successfully to map variability of soil salinity across a field, but although correlation exists between apparent EC and sulfate-bearing materials, it is not sufficiently strong to serve as a good predictor for conditions surrounding lime-induced heave in soil.

ACKNOWLEDGEMENTS

First and foremost, I extend my gratitude to Dr. Hallmark. He served as an outstanding mentor during the course of my master's program. His willingness to assist me in any way possible went above and the beyond the call of duty. To the rest of my committee members; Dr. Morgan for her remarkable patience in teaching me the art of spatial statistics and for being a friend, Dr. Feagley for his never ending positive attitude towards me and my work, and Dr. Searcy for introducing to me the ways of the EM38. I couldn't have asked for a better graduate committee to work with at Texas A&M University.

The support of the Natural Resources Conservation Service was continual during my research, as they assisted in providing me a sampling area that would fit the criteria necessary for my research. In addition, they provided me with elevation measurements and contour maps to incorporate in my thesis. They were always accurate, efficient, and enjoyable to work with.

I could not have completed my work without the timely and accurate work of the Soil Characterization Laboratory. Not only were my samples analyzed in superior fashion, the staff was extremely friendly and patient with me as I learned the procedures used in the laboratory. I cannot thank Donna Prochaska, Travis Waiser, Matt Piazza, Shane Waiser, and Adrean Roberson enough.

My statistical support team deserves a round of applause as well. Trent Fox, my husband, answered nearly every statistical question I threw at him. His daily support has made this process much easier. I am glad we made this journey together and believe it has made a strong foundation for the rest of our lives.

I thank my parents, Bob and Renee Hoffman, for getting me to this point in my life. Even though they don't always understand what I am working on, I could not have gotten this far without them. To my sister, Kara and brother, Nathan, thanks for helping me get through being homesick for Kansas and for providing me with a laugh whenever it was much needed.

Finally, thanks to Cowboy and Rowdy for just being you. A dog's unconditional love and slobbery tongue can remind you that life is not so bad after a rough day.

TABLE OF CONTENTS

Page

Page

LIST OF TABLES

LIST OF FIGURES

INTRODUCTION

Soil stabilization is performed to improve soil materials which would otherwise be unsuitable for road construction. The overall goals of soil stabilization are to increase stability and bearing capacity, increase resistance to weathering and erosion, and decrease the permeability of the material (Sherwood, 1993). This is commonly accomplished by using products such as hydrated lime ($Ca(OH)_2$) and quicklime (CaO) along with heavy equipment for soil compaction.

In the last few decades, a negative relationship between soils stabilized with lime products and the presence of sulfate mineral within that same soil has been recognized. The relationship can occur in two different media, the concrete itself or the soil bed. First, sulfates in the soil solution react with hydrated lime incorporated in the soil to be stabilized to form calcium sulphoaluminate, more commonly known as ettringite (Hunter, 1988). Ettringite can also form when sulfate ions become available within the concrete pore solution, either through diffusion of sulfate ions in the concrete from the outside or through internal sources (US Department of Transportation, 2002). In this scenario, ettringite formation occurs when sulfate ions attack the calcium hydroxide and alumna-bearing phase of the hydrated cement paste (US Department of Transportation, 2002). Ettringite occupies a greater volume than

_____

This thesis conforms to the style of the Soil Science Society of America Journal.

the combined volume of its reactants, leading to lime induced heave (Hunter, 1988). Millions of dollars are spent annually on repairing roads and highways that have deteriorated from lime-induced heave in sulfate-bearing soils, yet neither a cause nor resolution has been concisely determined.

The use of electromagnetic induction can potentially allow those involved in engineering and constructing roads to locate areas of sulfate-bearing soils accurately and efficiently. Once threshold levels of sulfate minerals have been located, potentially hazardous materials can be avoided, reducing deterioration of roadways and long-term repair costs.

The objectives of this research are to: 1) document soil solution electrical conductivity (EC) variability within selected sites that are high in sulfate-bearing materials, and 2) determine if electromagnetic induction is an efficient solution to locating threshold levels of sulfate-bearing materials using EC measurements collected with electromagnetic induction. Meeting these objectives should lead to strategies that ultimately reduce costs spent on repair and upkeep of roads by avoiding soils with elevated levels of sulfate during highway construction.

REVIEW OF LITERATURE

Soil Stabilization

Soil is a readily available material that is highly variable and ranges greatly in its suitability for stabilization. Stabilization is a process used to alter soil so that it is suitable for construction. The main techniques used for stabilization include mechanical stabilization and stabilization by the use of a stabilizing agent (Sherwood, 1993). An example of mechanical stabilization would include penetrating the soil with deep foundations, such as pile foundations. This research will focus on the latter of the two as it includes the use of hydrated lime and quicklime as a stabilizing agent.

According to Sherwood (1993), stabilization with a stabilizing agent may be implemented three ways: bonding soil particles together, waterproofing soil particles, and by the combination of bonding and waterproofing soil particles. These can be carried out via a physical reaction, chemical reaction between two chemicals, or a chemical reaction between the soil and a stabilizer (Sherwood, 1993). A chemical reaction between the soil and a stabilizer use products such a hydrated lime and quicklime. These products are granular or powder and usually are applied to the soil in their solid form (Sherwood, 1993). Typically, the amount of lime used to amend soil is in the range of 2 to 10% by weight (Powrie, 1997). Economically speaking, quicklime is more cost effective in terms of transport and handling, because hydrated lime contains about 25% water (Powrie, 1997).

The main benefits of lime stabilization include increased stiffness and durability, and volume stability as the soil becomes less susceptible to shrinking and swelling (Powrie, 1997). Powrie noted that the addition of lime to clay will improve its workability because the water content at the plastic limit is increased, and the clay becomes more friable. The shear strength (the strength resistant to the stresses on each face that act parallel to the face and at right angles to one another) will also increase as a result of the chemical bonding or cementation of soil particles (Powrie, 1997).

Lime stabilization occurs in a four-step process. The first step influences cation exchange capacity. Sodium and H^+ ions are replaced with Ca^{2+} from the liming material (Hunter, 1998; Sherwood, 1993). In the second step, clay particles flocculate, decreasing the plasticity index of the soil (Hunter, 1988). During these first two steps, free water is removed from the soil by the liming material, and heat is produced by the exothermic reaction, inducing drying (Sherwood, 1993). The next two steps encourage the cementation of the stabilized soil, which includes carbonation reactions and pozzolanic reactions (Hunter, 1988). Pozzolanic reactions lead to the final cementing process and occur once silica and alumina become available from the dissolution of clay particles at a pH above 10.5 (Hunter, 1988). Powrie (1997) states that an increase of the specific surface area of the soil particles increases the effectiveness of the cementation process, and available silica limits the degree of cementation. Pozzolanization is a slow, highly temperature dependent

process and the pozzolanic mechanism is the only process affected by the presence of sulfate, potentially resulting in lime-induced heave (Hunter, 1988).

Soils with the potential for treatment with lime are characterized as having at least 25% of the soil material pass through a 0.075-mm sieve, a plasticity index of at least 10, less than 1% by weight organic material, and soluble sulfates less than 0.3% (Little, 2000). In the state of Texas, approximately 26,250 miles of roadway have been built on lime-stabilized soil containing sulfate material (Texas Transportation Institution, 2003). The number one location of roads built on sulfate-bearing soils is the Texas Department of Transportation's Dallas District. It has been estimated that an annual savings of 10.5 million dollars would be possible if these areas were avoided (Texas Transportation Institution, 2003).

Calcium Sulfoaluminate – Ettringite

Ettringite, a hydrated calcium aluminum sulfate ($Ca_6Al_2(SO_4)_3(OH)_{12} \cdot 26H_2O$), forms in nature as a precipitate under hydrothermal conditions (Amethyst Galleries, Inc., 1996). Ettringite is a member of the Sulfate class of minerals, is bright yellow or white in color, has a vitreous luster, poor cleavage, and a specific gravity of 1.7 (Amethyst Galleries, Inc., 1996). Ettringite forms quickly and is a stable mineral in ambient conditions (Sabry et al., 1981).

The formation of ettringite in concrete does not always result in a negative scenario. If ettringite forms before the concrete has hardened, before pozzolanic reactions have occurred, it increases the stabilization of concrete. A

problem with ettringite formation arises when secondary ettringite forms after concrete has hardened, and is commonly referred to as delayed ettringite formation (DEF). The structural effects of DEF can reduce the life of concrete by causing expansion, loss of structural stiffness due to excessive cracking, and an increase in permeability which results in an increase in the rate of deterioration (Merrill, 1998).

The exact cause of DEF is unknown, but hypotheses abound. Some of the factors believed to encourage DEF include: heat treatment at higher temperatures, influence of freeze-thaw cycles, carbonation processes, and moisture effect (Stark and Bollmann, 1998). Two potential mechanisms may result in the formation of ettringite in hardened concrete: 1) additional ettringite formation by internal sulfate release, or 2) dissolution, transport, and recrystallization of existing ettringite (Stark and Bollmann, 1998).

Additional ettringite formation may occur when sulfate, locked in the concrete, reacts with moisture and aluminates over time resulting in a delayed formation of ettringite (Merrill, 1998). The second mechanism of ettringite, mobilization and recrystallization, occurs with elevated temperatures from hydration and/or curing. The elevated temperature causes ettringite to decompose into monosulfoaluminate ($3CaO{\cdot}Al_2O_3{\cdot}CaSO_4{\cdot}18H_2O$), then moisture and lower temperatures cause the ettringite to reform (Merrill, 1998).

For ettringite to form, the soil environment should have a water-soluble sulfate concentration greater than 5 g kg^{-1} and a strongly alkaline reaction of

greater than 12.3 (Fanning et al., 2002). The soil pH can easily reach 12.3 if the soil is initially calcareous and hydrated lime is added. Clay minerals dissolve in such environments, providing a source of silica and alumina available for the formation of thaumasite ($Ca_6[Si(OH)_6]_2(SO_4)_2(CO_3)_2 \cdot 24H_2O$) and ettringite, respectively (Fanning et al., 2002). When combined with an oxidation-hydration-dehydration process, these properties provide for optimum formation of ettringite. Ettringite requires a relatively low Al to Ca ratio; therefore, it does not require an extensive lime-silicate reaction for ettringite to capture a great deal of available Ca (Sabry et al., 1981). Since only small amounts of Al are needed for ettringite formation, it is difficult to stabilize lime-treated soils that contain sulfates.

Thaumasite, a mineral with characteristics similar to ettringite, is formed as a result of ettringite transformation. Ettringite always forms first and then slowly converts to thaumasite at temperatures below 15 °C (Hunter, 1988). Above 15 °C, ettringite remains stable (Hunter, 1988). It is not clear whether the damage caused to concrete is a result of ettringite or the transformation of ettringite to thaumasite, but both of these minerals are commonly found at sites of lime-induced heave (Hunter, 1988). Documentation of these minerals dates to as early as 1874, but as stated before, they have gained greater attention in the last 30 years.

Properties of Electromagnetic Induction

Electromagnetic induction is a method of measuring apparent soil EC by inducing an electrical current in the soil (Doerge et al., 2003). Soil EC is the measure of the soil's ability to conduct electricity measured in mS m^{-1}, and is primarily dependent upon soil properties, such as clay content, clay type, moisture, salinity, and temperature (Doerge et al., 2003). Soil properties such as cation exchange capacity, solum depth and pore continuity may also be extrapolated from apparent EC measurements.

Currently, the two most popular commercial instruments available for making apparent EC measurements are made by Geonics Limited (Mississauga, Ontario, Canada) and Veris Technologies (Salina, KS). The key difference between the two instruments manufactured by these companies, is that the Geonics Limited instrument measures apparent EC non-intrusively. The Veris instrument has coulters that must be dragged through the top few centimeters of the soil.

The electromagnet used to conduct this research was the EM38 model produced by Geonics Limited (Fig. 1). The EM38 is a lightweight, bar-shaped unit approximately 1-m long, is powered by a 9-V battery, and has a digital readout of apparent EC in mS m^{-1}. The principal theory of operation of the EM38 is shown in Fig. 2. The transmitting coil induces a magnetic field that varies in strength with soil properties that conduct electrical currents (Davis et al., 1997). A receiving coil reads the primary current and the secondary current

induced in the soil. The ratio between the primary and secondary current is related to apparent soil conductivity (Davis et al., 1997). Figure 2 shows the response of the EM38 measurement to different combinations of soil textures. When a clay horizon is closer to the surface (Fig. 2b), a higher reading is produced than (Fig. 2a) when a clay horizon is deeper in the profile.

Fig. 1. The EM38 produced by Geonics Limited (Ontario, Canada). The unit is demonstrated in the vertical dipole position.

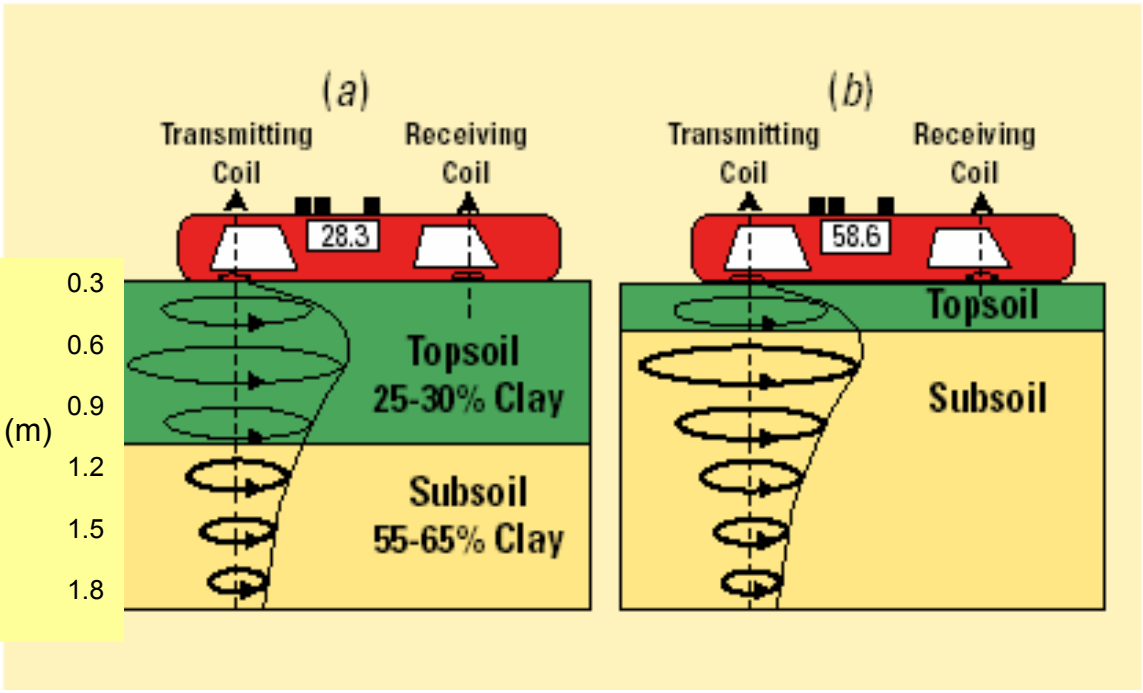

Fig. 2. The EM38 principle of operation in soils (Source: Davis et al., 1997).

The EM38 is designed for shallow applications specifically within the agricultural root zone (0.3 to 1.5 m) (McNeill, 1980). The depth that an instrument can measure apparent EC is dependent on the intercoil spacing and orientation of the electromagnet. Increasing the spacing between the transmitter coil and receiver coil extends the depth of penetration (Doolittle et al., 2002). The intercoil spacing of the EM38 is fixed at 1 m limiting its maximum response depth to 2 m depending on soil conditions (McNeill, 1980).

The EM38 has two coil orientations, vertical dipole and horizontal dipole, which allows measurements at different depth intervals. The horizontal dipole orientation is more sensitive to differences in apparent EC and can measure to a maximum depth of approximately 0.75 m (McNeill, 1980). The vertical dipole orientation is more responsive to differences occurring at a greater depth and can measure apparent EC to a maximum depth of 1.5 m (McNeill, 1980). The graph shown in Fig. 3 emphasizes the manner in which the different dipole modes respond to material at different depths. For both the vertical and horizontal dipole position, the EM38 reading is an integration with depth of the apparent bulk soil EC.

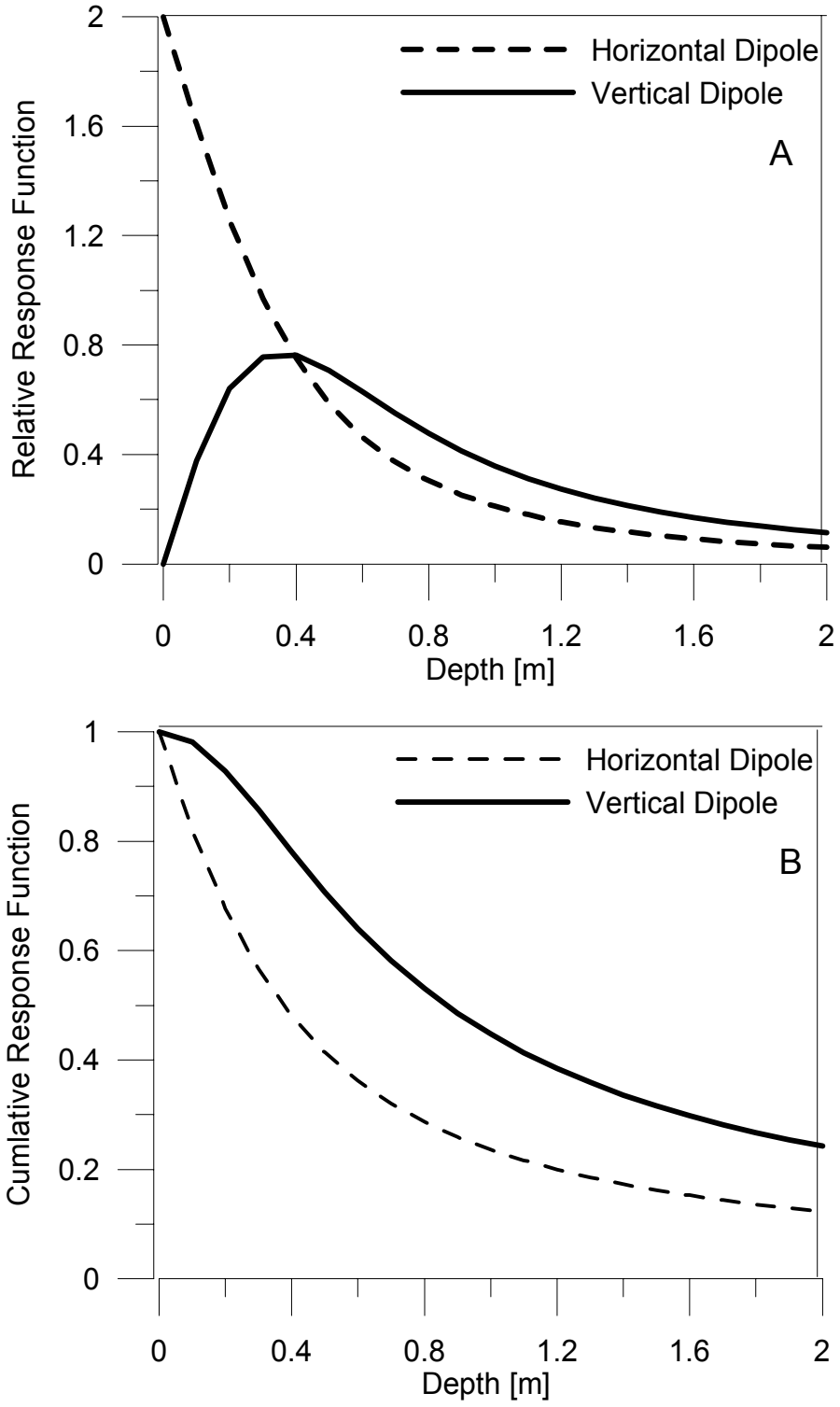

Fig. 3. The EM38 response versus depth for vertical and horizontal dipoles: A)Relative, and B)Cumulative (McNeill, 1980).

As previously stated, soil EC is the measure of the soil's ability to conduct electricity dependent upon soil properties, such as clay content, clay type, moisture, and salinity. Equation [1] shows how each of these factors contributes to the apparent EC response of the EM38, where EC_w is conductivity of the soil water, θ is volumetric water content, a is clay content, b is clay type, and EC_s is a bulk surface electrical conductivity (Rhoades et al., 1976).

$$\text{Apparent EC} = EC_w\theta(a\theta + b) + EC_s \qquad [1]$$

In this study, soluble salts, clays, and water content in the soil system would be expected to contribute to the apparent EC reading. Soluble salts commonly include cations such as, Ca^{2+}, Mg^{2+}, Na^{+}, and K^{+} and anions such as Cl^{-}, HCO_3^{-}, CO_3^{2-}, NO_3^{-}, and SO_4^{2-} (Jurinak, 1990). Soils developing from marine sediments such as soils of the Blackland Prairies (Hallmark, 1993) would be expected to contain some salts, especially in lower horizons. Soil data from Hallmark et al. (1986) show Vertisols of the Blackland Prairies commonly contain gypsum and soluble sulfates when developing from marine deposits. Therefore, if much of the variability in salinity is associated with sulfates, the EM38 may satisfactorily indicate areas of higher sulfate concentration. Increase in salts in this area might cause higher EM38 readings, which could be used to establish a correlation between apparent EC and sulfate concentration.

Any metal may interfere with electromagnet measurements, including power lines, fencing, metal buildings, and the vehicle used to transport the electromagnet when it is in use. When using the EM38, calibration is important

and should be done as often as every 0.5 h on highly resistive soils. Calibration, or zeroing, should always be done at the same location for each survey.

Geostatistics

If variation in a soil property is random, sample values are not a function of sample separation distance, and classical statistics are sufficient for analyzing data (Mulla, 1989). For most soils this is not the case; instead, samples that are obtained from closely spaced locations are more similar to each other than samples separated further apart (Mulla, 1989). Because classical statistics do not account for the relationship between the value of a sample and its location in a field, geostatistics must be used to describe patterns in spatial variability. The term geostatistics is used to describe a set of statistical tools that are extensions of classical statistics without the assumption of sample independence (Upchurch and Edmonds, 1991). In addition to classical statistics, geostatistics were used to examine the data collected for this research.

The geostatiscal procedure used involves computing the semivariance of the data, fitting semivariogram models to the semivariance data, and producing a detailed spatial map utilizing this data and a process know as kriging to predict intermediate points of unknown values.

According to Burgess and Webster (1980), semivariance is the measure of similarity, on average, between points a given distance apart. Equation [2] defines semivariance [$\gamma(h)$] for an empirical semivariogram where $N(h)$ is equal to the number of samples separated by a distance h, $Z(x_i)$ is equal to the value

of the measured property at location x_i, and $Z(x_i+h)$ is the value of the measured property at location x_i+h (Nielsen and Wendroth, 2003).

$$\gamma(h) = [1/(2N_h)] \sum_{i=1}^{N_h} [Z(x_i) - Z(x_i+h)]^2 \qquad [2]$$

Equation [3] (Cressie, 1993) defines semivariance for a robust fit variogram. Robust fits are used when there are outliers present or data are severely skewed (Cressie, 1993).

$$\gamma(h) =[1/(2N_h) \sum_{i=1}^{N_h} [Z(x_i) - Z(x_i+h)]^{0.5}]^4 \qquad [3]$$

The basic tool of geostatistics is the semivariogram, which expresses the sample's degree of dependence in reference to where it is located within the population (Upchurch and Edmonds, 1991). The semivariogram reveals the nature of the geographic variation of interest and is needed to provide kriging estimates at previously unrecorded points (Burgess and Webster, 1980). Semivariograms can be produced using a linear (Eq. [4]), spherical (Eq. [5]), exponential (Eq. [6]), power (Eq. [7]), or Gaussian model (Eq. [8]) (Nielsen and Wendroth, 2003).

$$\gamma(h) = C_0 + mh \qquad [4]$$

$$\gamma(h) = C_0 + C_1 [1.5(h/a) - 0.5(h/a)^3] \qquad h<a \qquad [5]$$

$$\gamma(h) = C_0 + C_1 [1 - \exp(-h/a)] \qquad [6]$$

$$\gamma(h) = C_0 + mh^a \qquad [7]$$

$$\gamma(h) = C_0 + C_1 [1 - \exp(-h/a)^2] \qquad [8]$$

The nugget, sill, and range are parameters used to define a semivariogram (Mulla, 1989). The nugget (C_0) is the value at the Y-axis intercept and is a measure of unexplained variance (Mulla, 1989). The sill (C_1) is the value at which the model plateaus and is approximately equal to the sample variance. Linear and power models will not plateau because of being unbounded (Nielsen and Wendroth, 2003). The range (a) is the distance at which the sill is reached, and indicates the distance at which the data becomes spatial independent. Other important variables included in the semivariogram models are distance between sample locations (h) and slope (m).

An objective function value is calculated to evaluate the goodness of fit of the semivariogram model to the semivariogram data. The semivariogram model that provides the lowest objective function value provides the best fit for the data (Creisse, 1993). Figure 4 shows an example of a semivariogram, the semivariogram model, and the model's parameters.

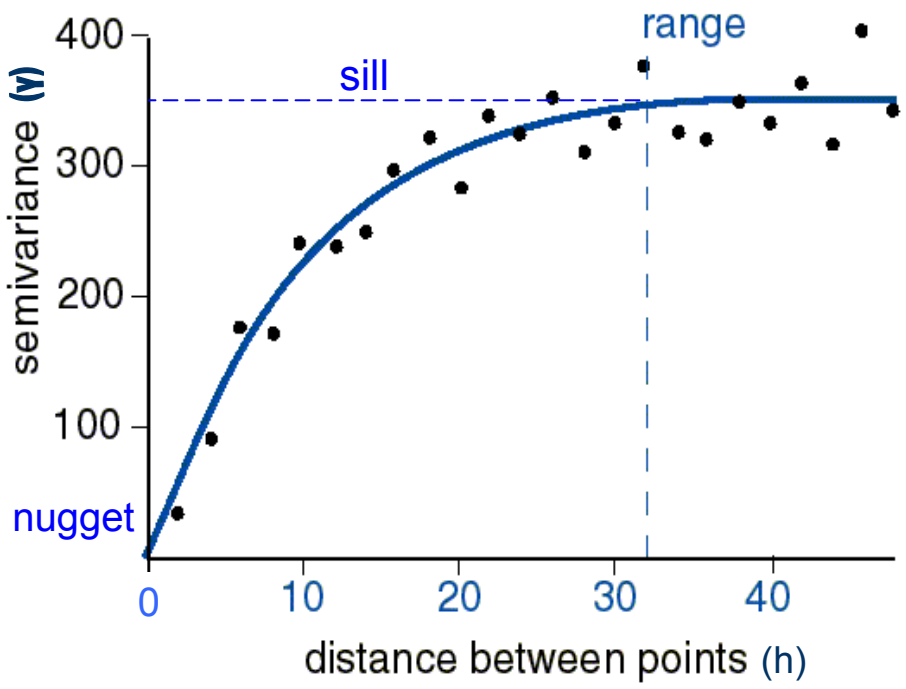

Fig. 4. Semivariogram and its parameters.

Once spatial dependence has been modeled, values for points in a field that have not been measured can be predicted. Interpolating between sampled points using a semivariogram is known as kriging (Upchurch and Edmonds, 1991). Kriging is a form of weighted local averaging that is optimized by the semivariogram model and provides values at unrecorded places without bias (Burgess and Webster, 1980).

Another method of kriging, which was used in this research, is simple regression kriging. If a regression model between points and high-resolution survey data can be fit, and the residuals of this regression model are not spatially correlated, simple regression kriging can be used to interpolate the point data using survey data. The spatial independence of the regression model residuals is tested by plotting the semivariance of the residuals. If pure nugget effect exists, then the residuals are spatially independent. To interpolate the point data, the survey data are first kriged, then the survey data are converted to the point data using the regression model.

METHODS

Site Information

The sampling area for this study is located in the Blackland Prairies Land Resource Area and more specifically, a 0.43-ha plot in Bell County, southeast of Temple, TX (31° 6'N, 97° 21'W). The area was part of the Soil Survey of Bell County (Huckabee et al., 1977) and was mapped as predominately Houston Black, clay, a fine, smectitic, thermic Udic Haplustert. The soil was known to contain gypsum prior to conducting this research. The research plot also contains a small area of Heiden-Ferris complex in the northwest quarter. The Heiden series is a fine, smectitic, thermic Udic Haplustert and the Ferris series as a fine, smectitic, thermic Chromic Udic Haplustert (classifications found at http://soils.usda.gov/soils/technical/classification/osd/index.html).

The Houston Black series consists of nearly level to gently sloping, calcareous, clayey, deep soils on uplands, which were formed under prairie vegetation in marine clays and marls. These soils are moderately well drained, with very slow permeability, and high available water holding capacity. Because these soils are Vertisols, in undisturbed areas the gilgai microrelief can be seen and consists of knolls that are approximately 7.5 to 38 cm higher than

depressions. The distance between the center of the knolls and the center of the depressions ranges from 1.8 to 3.7 m. When dry, these soils exhibit cracks from the surface that extend to a depth of more than 1 m. Houston Black soils are commonly used to produce crops of grain sorghum, cotton, corn, small grains, and forage grasses.

Grid Design

The plot selected for this study was 45 m X 95 m. A sampling grid with 5-m spacings was superimposed on the plot allowing for 200 observations to be made. A barbed wire fence was located 9.8 m west of the grid and ran the length of the grid. High voltage power lines were located along the north side of the grid approximately 85 m away from the northwest corner of the field and 50 m from the northeast. These were noted because of their possible interference with the apparent EC readings. Figure 5 shows the layout of the grid and its surrounding features.

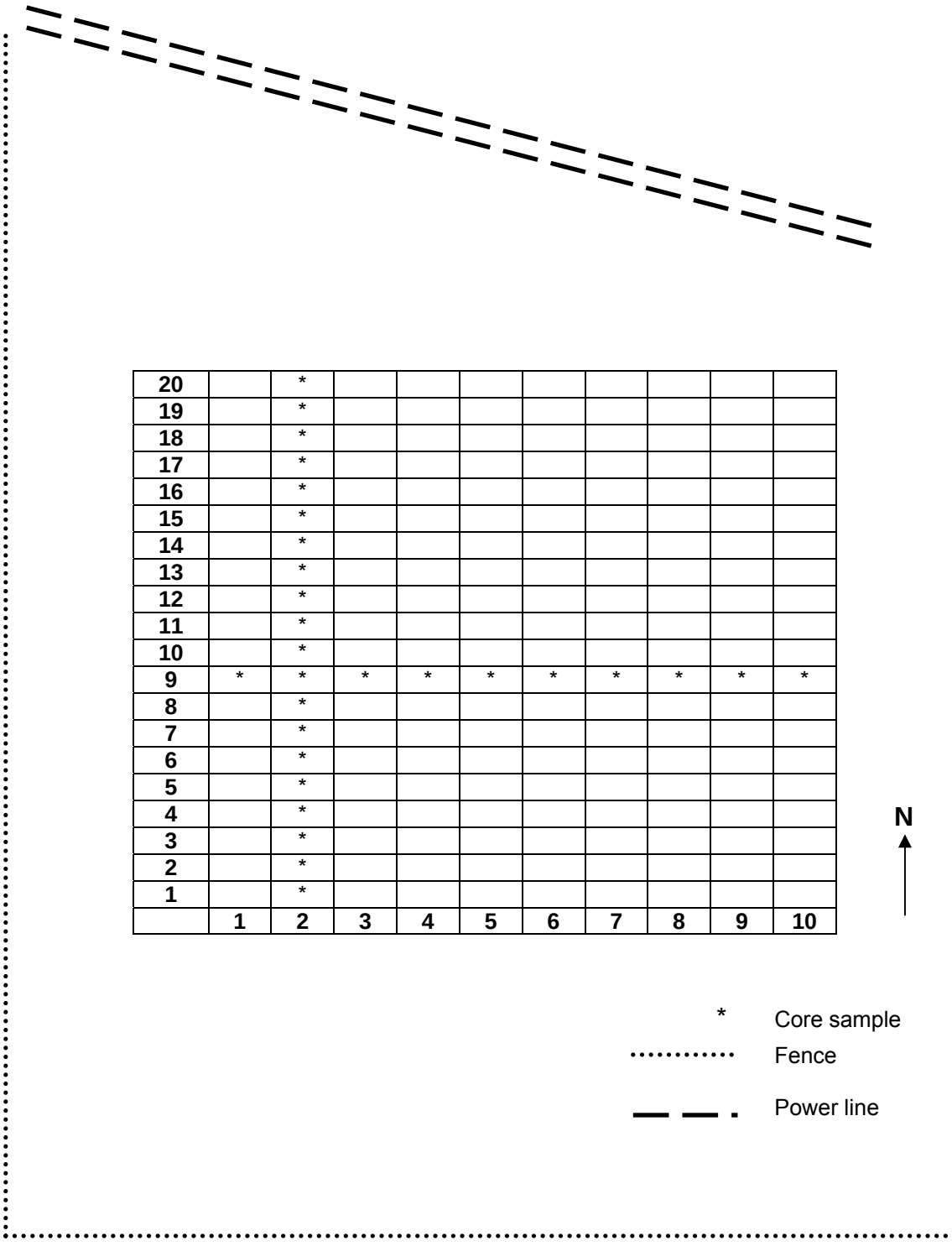

Fig. 5. Grid design.

EM38 Calibration

Apparent EC using the EM38 was measured on July 22, 2003 and November 13, 2003. To eliminate significant problems with drift of the instrument, the EM38 was calibrated at the beginning of each transect, checked at the end of each transect, and then recalibrated before the start of the next transect. Calibration was done at the same location each time and followed the calibration procedure suggested by Geonics Limited (2002).

Steps for calibration include the initial inphase nulling, instrument zero, and final inphase nulling. A stand constructed of PVC pipe was used to elevate the instrument to a height of 1.5 m when required in the calibration instructions. To complete the initial inphase nulling, the instrument's inphase (I/P) range is set to 1,000 mS m^{-1}, and the instrument is lifted to a height of 1.5 m and placed in the horizontal dipole mode. The I/P meter is nulled to indicate zero by first adjusting the I/P coarse zero and then the I/P fine zero control. This procedure is repeated again after the I/P range is switched to 100 mS m^{-1}. The inphase initial nulling is considered satisfactory when the instrument at a height of 1.5 m reads 0 plus or minus 10 mS m^{-1} in the 100 mS m^{-1} range of the I/P mode.

The instrument zeroing step requires that the instrument be lifted again to a height of 1.5 m. With the instrument in the horizontal dipole mode of operation and the quadphase (Q/P) range set to 100 mS m^{-1}, the Q/P zero control is adjusted so the Q/P meter reads approximately 50 mS m^{-1}. Without changing the height, the instrument is rotated to the vertical dipole orientation, and the Q/P

meter is read. This reading should be twice that of the reading in the horizontal dipole, indicating that the zero is correctly set. This process is repeated until the vertical reading is double the horizontal reading by adjusting the fine and coarse zero controls.

The final inphase nulling requires the instrument to be placed on the ground in the position that the survey will be conducted, horizontal or vertical. Once in the appropriate position, the procedure described for initial I/P nulling is completed again.

Field Collection

The grid was walked, and observations were taken by resting the EM38 on the soil surface in the vertical dipole mode of operation until a stable reading was recorded manually. Upon completion of the apparent EC data collection in July, selection of one N-S transect and one E-W transect was made that appeared representative of the entire field. Specifically, column 2 (N-S) and row 9 (E-W) were selected to represent the variation of the field, because they had high, low, and intermediate EC values. Soil cores with a 5 cm diameter were taken to a depth of 1.5 m at each of the 29 sample locations (point data), as it was not feasible to obtain a core sample at each of the 200 points. Soil physical characteristics of each soil core were recorded including depth to gypsum, presence of calcium carbonate, thickness of A horizon to suggest position of microrelief, and depth to shale. Cores were divided into three samples based

upon depth: 0 to 25 cm, 25 to 75 cm, and 75 to 150 cm. Samples were sealed in plastic bags to preserve moisture until moist weights could be recorded.

Apparent EC determinations were taken again on November 13, 2003 when soil moisture content was expected to be higher than the July soil moisture. The November measurements were taken to investigate the influence of soil moisture on the variation in apparent EC, and to determine which moisture state might be more conducive to evaluating sulfate content with apparent EC. Again, 29 cores were taken in the same locations (within 20 cm) as the July samples. Cores were divided at the same depths as in July and placed in sealed plastic bags until moist weights could be taken.

After the second sampling period, elevations of each point were recorded using a laser level system provided by and assisted by the Natural Resources Conservation Service.

Moisture Content

Samples were weighed immediately upon arrival at the Soil Characterization Laboratory to accurately record moist weights of the soil samples. After recording the moisture, the samples were air-dried and weighed again to calculate percent moisture on an air-dried basis. Equation [9] was used to complete calculations on an air-dried basis after the weight of the storage bag was subtracted from each subsample.

$$\text{percent moisture (air dried)} = [(\text{moist soil weight (g)} - \text{air-dried soil weight (g)}) / \text{air-dry soil weight (g)}] \times 100 \quad [9]$$

A corrective moisture factor was determined for each sample by taking 10 g of ground (<2 mm diameter) air-dried soil and oven-drying it at a temperature of 105°C. The moisture factor was calculated using Eq. [10] after the weight of the container was subtracted. This factor was used to convert air-dried moisture content to an oven-dried basis shown in Eq. [11].

$$\text{moisture factor} = \text{air-dried soil (g)} / \text{oven-dried soil (g)} \quad [10]$$

$$\text{percent moisture (oven-dried)} = [(\text{moisture factor} - 1) \times 100] + \text{percent moisture (air-dried)} \quad [11]$$

Electrical Conductivity and Soluble Cations of the Saturated Paste Extract

Following the Soil Survey Laboratory Methods (Soil Survey Laboratory Staff, 1996), a saturated paste extract was made for all 87 samples taken in July. The procedure involved weighing 200 g air-dried soil and adding distilled water until the saturation point was reached (when the soil begins to flow). The saturated soil was allowed to sit overnight and then weighed prior to extraction. The paste was transferred to a filter funnel fitted with Whatman No. 42 filter paper, and a syringe was attached to the outflow end of the filter funnel. The extraction was done over a 2 h period, and then the extract was transferred to a plastic storage bottle. The stored extract is refrigerated until analyses were completed. The extract was warmed to room temperature before each analysis.

Electrical conductivity was determined on the saturated paste extract and recorded in dS m^{-1}. Then, the extract was analyzed for soluble cations. An

aliquot of extract was diluted 1:10 with distilled water, then Na^+ and K^+ were measured using a Varion Spectra AA 55 unit via flame emission mode using an acetylene-air flame. If a reading was obtained that was above the highest standard, a greater dilution was used. For Ca^{2+} and Mg^{2+}, a fresh aliquot of extract was prepared by diluting 1:10, and they were detemined using atomic absorption with an acetylene-nitrous oxide flame. Soluble cations, Ca^{2+}, Mg^{2+}, K^+, and Na^+, were expressed in units of mmol (+) L^{-1} in the saturated paste extract.

Soluble Anions of the Saturated Paste Extract

Analyses of carbonate, bicarbonate, and chloride were completed on the saturated paste extract of each sample according to methods described by the Soil Survey Laboratory Staff (1972). One aliquot of saturated paste extract was used for carbonate, bicarbonate, and chloride, as indicated in Table 1.

Table 1. Aliquot size for carbonate, bicarbonate, and chloride determinations.

EC	Aliquot Size
dS m^{-1}	mL
<10	5
>10	2

The aliquot was made to a volume of approximately 50 mL with distilled water. Two blanks consisting of distilled water alone were also prepared. Two

drops of phenolphthalein were added to each sample. If a pink color developed, the sample contained soluble carbonate and was titrated with 0.05 N H_2SO_4 until the pink color disappeared. Samples of this study did not contain soluble carbonate.

Four drops of methyl orange indicator were then added to each sample, and the solution was titrated with 0.05 N H_2SO_4 to the methyl orange endpoint (orange color). This acid-base titration determines the volume of acid used to quantify the amount of bicarbonate in each sample. Bicarbonate concentration was then calculated using Eq. [12].

bicarbonate (mmol (-) L^{-1}) = (mL H_2SO_4 sample – mL H_2SO_4 blank) X (N H_2SO_4) X (1000) / aliquot volume [12]

To the same aliquot and blanks titrated for the carbonate and bicarbonate procedure, 6 drops of K_2CrO_4 were added. The sample was titrated with 0.05 N $AgNO_3$ until a reddish endpoint was reached. This titration allows for Ag^+ to react with Cl^- in the sample and precipitate out as a white precipitate. Once all the Cl^- has precipitated, the Ag^+ then reacts with the CrO_4^{2-} producing a reddish precipitate that signals the endpoint of this titration. Equation [13] was used to calculate the Cl^- concentration as mmols (-) $L^{-1}$of each sample.

Cl^- (mmols (-) L^{-1}) = ((mL $AgNO_3$ sample – mL $AgNO_3$ blank) X N $AgNO_3$ X 1000) /aliquot volume [13]

Sulfate analysis was completed using the saturated paste extract and was determined using the procedure described by Jackson (1958). Aliquot size was based on EC of the saturated paste extract as indicated in Table 2. The

sample aliquot was transferred to a 25-mL volumetric flask and 0.5 g of $BaCl_2$ (powdered) was added to precipitate the SO_4^{2-} as $BaSO_4$. One mL of 6 N HCl with 1% gum acacia was also added to each flask in order to keep colloids in suspension long enough to determine turbidity. Each sample was brought to a volume of 25 mL, transferred to a cuvette, and turbidity determined using a turbidimeter.

Table 2. Aliquot size for soluble sulfate determination.

EC	Aliquot Size
dS m^{-1}	mL
< 1.0	2
1.0 – 2.5	1
2.5 – 5.0	0.5
> 5.0	0.2

A standard curve was made to convert turbidity readings into sulfate concentration as mmol (-) L^{-1}. Sulfate standards were made from a sulfate stock solution of 2.5 mmol (-) L^{-1}. Dilution of the stock solution gave concentrations of 0.1, 0.2, 0.5, 0.7, and 1.0 mmol (-) L^{-1} of sulfate standards. Standards were precipitated with $BaCl_2$ at the same time as samples. Tubidity of the samples and standards was determined, standard curves of standards versus readings were developed, and sample SO_4^{2-} concentrations were calculated by Eq. [14].

Sample SO_4^{2-} (mmol (-) L^{-1}) = (mmol (-) L^{-1} SO_4^{2-} from curve) X (25/mL aliquot) [14]

It should be noted that this method allows for approximately 80% of the sulfate to be recovered.

Percent Gypsum

Percent gypsum was determined using a procedure listed in the Soil Survey Laboratory Staff (1996). Twenty g of air-dried soil were weighed into a sedimentation bottle and 200 mL of distilled water added. A different ratio of soil to water was used if gypsum percentages were too high to be calculated (less soil to more water). The bottle was shaken overnight, and the solution was filtered using Whatman No. 42 filter paper. A 5-mL aliquot of filtrate was pipetted into a 15-mL conical centrifuge tube, 5 mL of acetone added and the water-acetone was mixed well. The mixture was allowed to stand for at least 10 min. The $CaSO_4$ precipitate was centrifuged at 2,000 rpm for 5 min. The supernatant liquid was decanted carefully, and the inverted tube was allowed to drain for 5 min. Another 5 mL of acetone was added to wash the precipitate, centrifuged again, decanted and drained. Then, 10 mL of distilled water were added to the $CaSO_4$ to dissolve the precipitate. The EC of the dissolved gypsum was then measured.

Using Table 3 from the Soil Survey Laboratory Methods Manual, gypsum content was determined. This value was then used in Eq. [15] and [16] to calculate percent gypsum.

percent gypsum (uncorrected) = (gypsum (mmols L^{-1}) X mL water X 0.08609 (g $mmol^{-1}$) X moisture factor) / (sample weight (g) X 5) [15]

percent gypsum (corrected) = percent gypsum (uncorrected) / (1 + (0.001942 X percent gypsum (uncorrected))) [16]

Table 3. Conversion of EC readings of soluble gypsum extract (mmhos cm^{-1}) to gypsum content (mmols 100 g^{-1} soil) (Source: Soil Survey Laboratories Staff, 1996).***

EC	0.00	0.01	0.02	0.03	0.04	0.05	0.06	0.07	0.08	0.09
0.0							0.40			
0.1	0.80	0.89	0.98	1.10	1.22	1.31	1.40	1.50	1.60	1.70
0.2	1.80	1.90	2.00	2.10	2.20	2.30	2.40	2.50	2.60	2.70
0.3	2.80	2.90	3.00	3.10	3.20	3.30	3.40	3.50	3.60	3.72
0.4	3.85	3.98	4.10	4.22	4.35	4.48	4.60	4.70	4.80	4.90
0.5	5.00	5.12	5.25	5.38	5.50	5.62	5.75	5.88	6.00	6.12
0.6	6.25	6.35	6.45	6.58	6.70	6.92	6.95	7.05	7.15	7.28
0.7	7.40	7.52	7.65	7.78	7.90	8.04	8.18	8.32	8.45	8.58
0.8	9.70	8.82	8.95	9.05	9.15	9.28	9.40	9.55	9.70	9.85
0.9	10.00	10.12	10.25	10.38	10.50	10.62	10.75	10.88	11.00	11.15
1.0	11.30									

***The EC of the soluble gypsum extract is in the row header in tenths and the hundredths of the reading is in the column header of the table. The gypsum content is the cell where the tenths row and the hundredths column intercept.

Classical Statistical Analysis

Regression and multiple regression were the main classical statistical procedures used for this research. Initially, a correlation matrix was developed among selected variables to reveal significant relationships using Pearson's Partial Correlation (SAS Institute, Inc., 1999). All relationships were calculated, but only soil properties that were significantly correlated to the apparent EC readings were the focus for further statistical analyses. When selected variables were significantly correlated ($p \leq 0.05$), stepwise multiple regression was performed. A depth-weighted average of the three values for each core was calculated, and for each of the correlated variables, stepwise multiple regressions were then completed. Finally, regressions were completed incorporating the three depths and calculating a sensitivity-weighted average for correlated variables.

Spatial Statistical Analysis

For this portion of statistical analysis, only significantly correlated properties with the EM38's apparent EC values determined from Pearson's Partial Correlation were used. Using each of these values and a geographical reference point, semivariance was calculated using the standard semivariogram Eq. [2] and using the equation for a robust variogram, Eq. [3]. Each empirical semivariogram was fit with all the models (linear, spherical, exponential, power, or Gaussian (Eq. [4] through [8]) and the best model fit was selected using the objective function value. The model that produced the lowest objective function

value was used to calculate a representative range, nugget, and sill. Simple regression kriging was used to predict values at locations in the field not measured. Maps were produced to illustrate these predicted values.

The S-Plus 6.0 Professional for Windows (2001) was the computer program used to calculate the semivariance, the models, and test regression residuals for spatial independence. Surfer 8 (2002) was used to krige the apparent EC data and convert that data using chosen regression models. Spatial maps were made once kriging was completed.

RESULTS AND DISCUSSION

EM38 Observations

The EM38 readings (apparent EC) collected on July 22, 2003 ranged from 73 to 125 mS m^{-1} with a mean of 99 mS m^{-1}. Observations recorded on November 13, 2003 ranged from 106 to 167 mS m^{-1}, with a mean of 133 mS m^{-1}. Figures A-1 and A-2, found in Appendix A, show all observations and their geographical position for each sampling date. Results in November were higher when compared to the July sampling date, because of the higher soil moisture content in November (data presented later).

Classical statistics were used to determine the strength of the relationship between apparent EC measurements taken with the EM38 in July and November. Figure 6 shows this relationship, which resulted in a strong correlation between the two measurements (r^2 = 0.72).

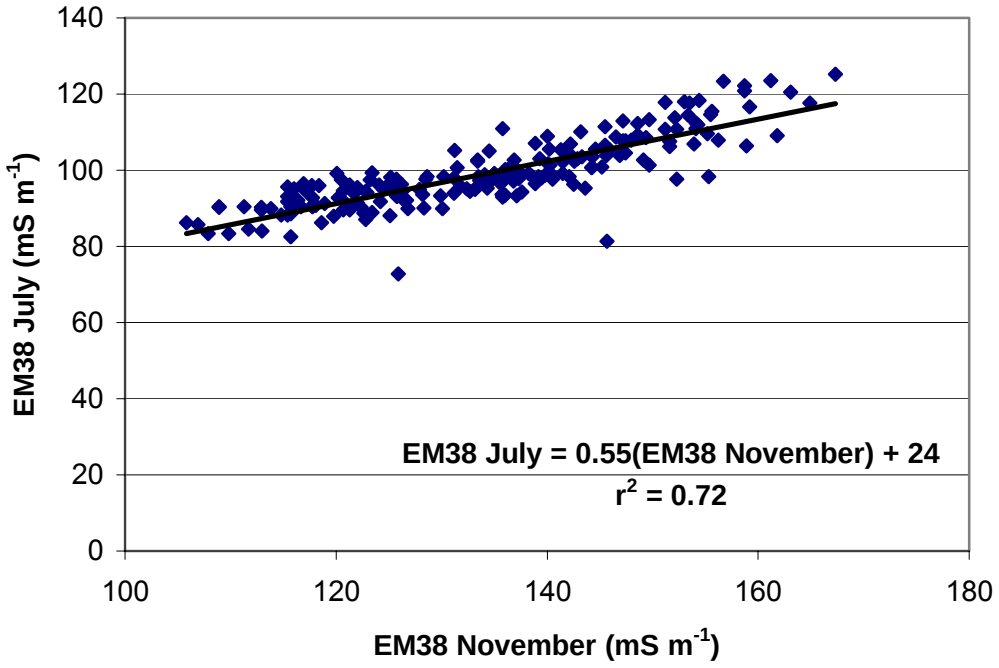

Fig. 6. Relationship between apparent EC measurements taken in July and November, 2003.

Semivariance of apparent EC values were calculated for each of the sampling dates (Figs. 7 and 8). These semivariograms are used to determine the nugget (measure of unexplained variance), sill (sample variance), and range (distance at which pairs are no longer correlated) for the apparent EC observed in the study area.

The July apparent EC data had a nugget of 8.8 $(mS\ m^{-1})^2$, sill of 92 $(mS\ m^{-1})^2$, and range of 52 m according to the spherical model fit. For the November sampling date, again using spherical model fit, the nugget is 0.52 $(mS\ m^{-1})^2$, the sill is 290 $(mS\ m^{-1})^2$, and the range is 60 m.

The July data showed that samples were spatially correlated through a range of 52 m, beyond which points were no longer spatially correlated. For the November data, points remained spatially correlated up to a distance of 60 m. The nugget was lower (0.52 (mS m^{-1})^2) than the July sampling period (8.8 (mS m^{-1})^2), which indicates less random measurement error. The additional observations in November at 1-m intervals, or the increase in moisture content may have contributed to the lower nugget. Location of these additional observations at 1-m intervals are shown as dotted transect lines in Fig. 9 for the November plot and their apparent EC values are found in Appendix A (Table on p. 62).

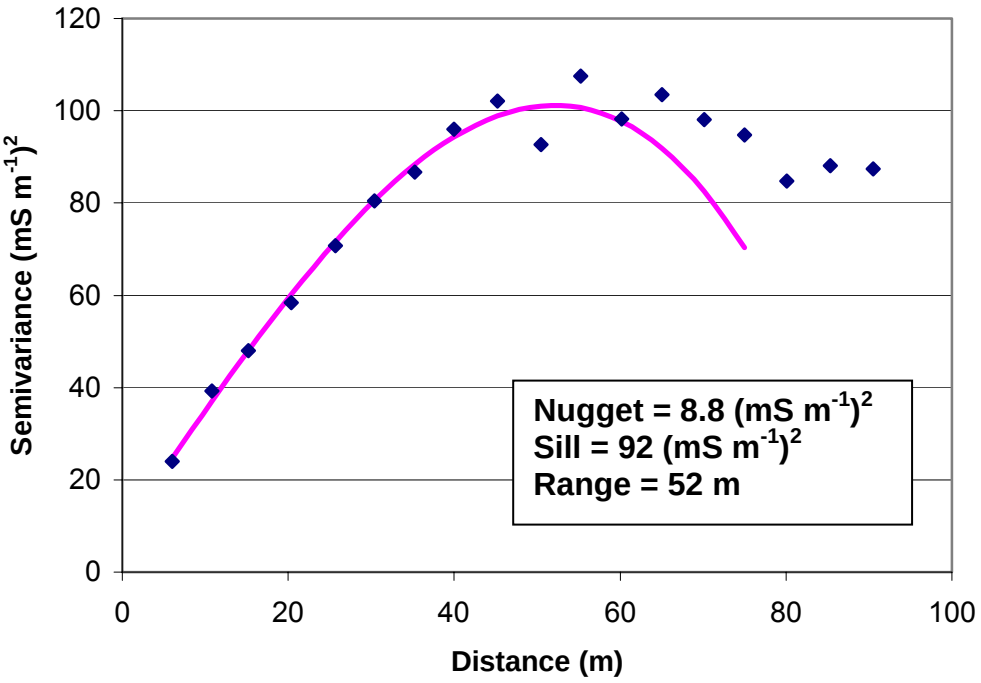

Fig. 7. Semivariogram for the apparent EC in July for the study area.

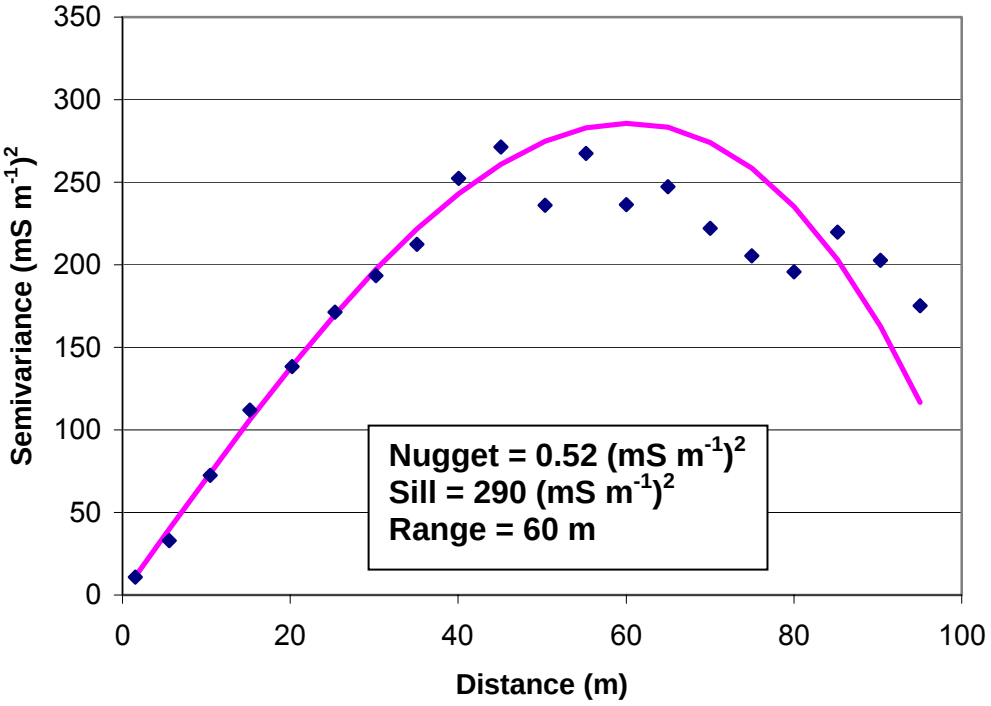

Fig. 8. Semivariogram for the apparent EC in November for the study area.

Using the EM38 data presented in Figs. A-1 and A-2, maps were produced (see Fig. 9) by kriging. Arrows along the axes of each map designate rows and columns from which soil cores were obtained. These maps of apparent EC show trends across the field. Apparent EC tended to be lowest in the southeast corner of the study area, and increased downslope toward the northwest. The apparent EC values were also high along the west boundary of the field. The influence of moisture content is evident, as the November map shows greater variability and overall higher readings across the field.

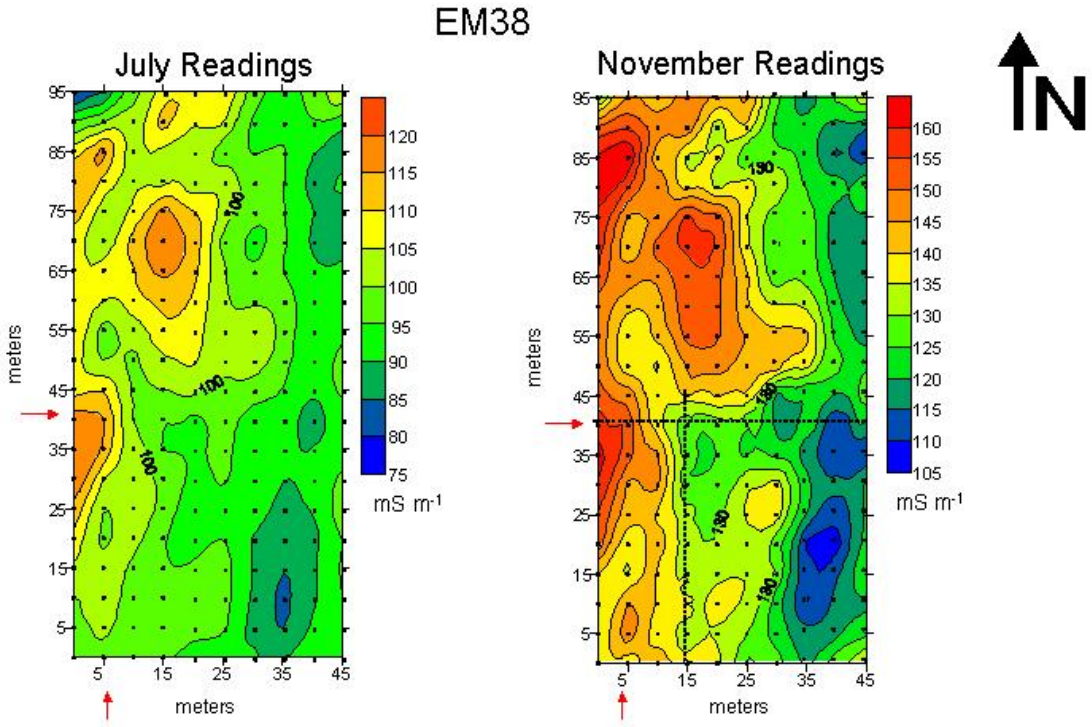

Fig. 9. Kriged EM38 readings (apparent EC mS m^{-1}) across the study area in July and November, 2003.

Elevation

To determine if there is a relationship between the EM38 readings and topography changes within the field, elevation for each of the 200 grid points was measured. The elevation of the study area is approximately 135 m above sea level. The change in elevation across the field is 5.1 m (range of 132.6 to 137.7 m) with the highest elevations located in the southeast corner of the study area and the lowest elevations in the northwest corner. The mean elevation for the field is 135.7 m, and the mean slope for the field is 3.1% over a distance of 1 m. Figure 10 shows a contour map of the area.

A simple regression analysis was used to determine if a statistical relationship existed between elevation and apparent EC as determined in July and November. It was found that the two are not significantly correlated ($p \leq 0.05$) and result in $r^2 = 0.16$ for July and $r^2 = 0.19$ for November.

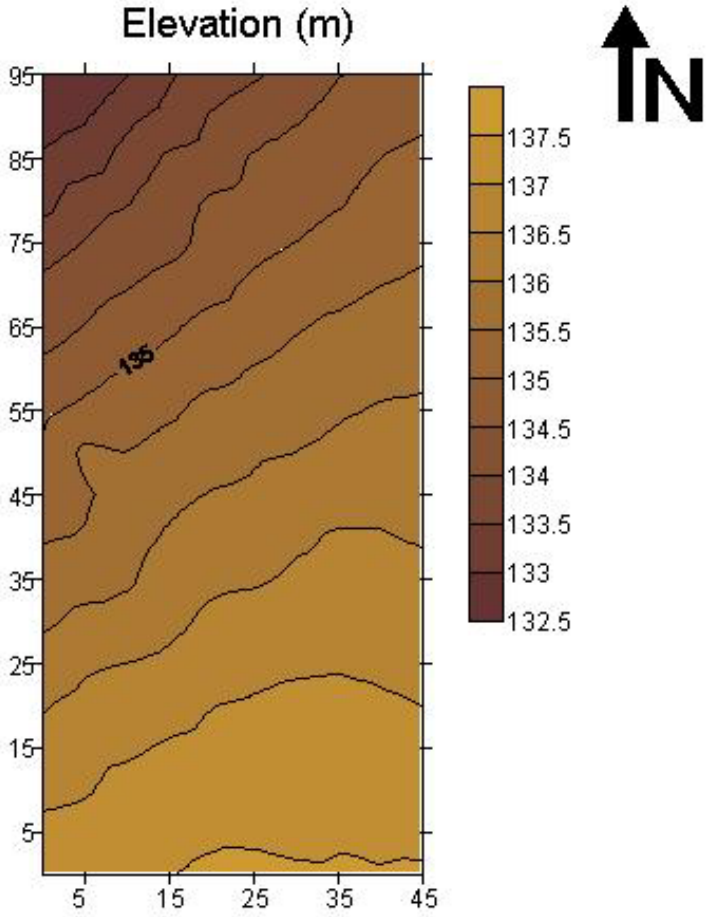

Fig. 10. Elevation (m) and contour map for the study area (contour lines are at 0.5 m intervals).

Laboratory Analyses

Laboratory analyses were completed for all core locations and included air-dried moisture content, oven-dried moisture content, EC of the saturated paste extract, soluble cations and anions of the saturated paste extract, and percent gypsum. Results from laboratory analyses can be found in Tables B-1 through B-5 in Appendix B.

Table 4 summarizes the minimum, maximum, and mean values of analysis completed for percent moisture content. The range of percent moisture content was much wider for samples collected in July than samples collected in November, and at each depth, the mean percent moisture is higher in November than July.

Table 4. Summary statistics for percent moisture content of cores taken in July and November.

Month	Depth	Oven Dry Moisture Content			
		Minimum	Maximum	Mean	Standard Deviation
	cm	----------%----------			
July	0-25	9.2	20.9	16.1[a]	2.9
July	25-75	8.1	24.6	17.9[b]	4.1
July	75-150	10.3	27.7	22.2[c]	4.2
November	0-25	19.2	25.2	22.8[c]	1.6
November	25-75	21.3	30.0	25.5[d]	2.5
November	75-150	20.6	28.6	25.6[d]	1.9

[abcd] Means without common superscript differ at $p \leq 0.05$.

Summary statistics for EC of the saturated paste extract are found in Table 5 and show that with increasing depth, an increase in EC occurs. The minimum, maximum, and mean determined for the third depth (75 to 150 cm) indicate that the soil in the entire study is saline below 75 cm as all samples have an EC above 4 dS m^{-1}.

Table 5. Summary statistics for EC of the saturated paste extract.

Depth	Electrical Conductivity			
	Minimum	Maximum	Mean	Standard
cm	----------dS m^{-1}----------			Deviation
0-25	0.5	2.3	1.0[a]	0.6
25-75	0.7	3.7	2.5[b]	0.8
75-150	4.2	6.3	5.4[c]	0.5

[abc] Means without common superscript differ at $p < 0.01$

Similar trends are exhibited for soluble SO_4^{2-} (mmol (-) L^{-1}), shown in Table 6. With depth the soluble SO_4^{2-} concentrations increases in the soil profile.

Table 6. Summary statistics for SO_4^{2-}.

Depth	Sulfate Concentration			
	Minimum	Maximum	Mean	Standard
cm	mmols (-) L^{-1}			Deviation
0-25	0.3	28.6	7.8[a]	8.8
25-75	2.8	39.2	23.2[b]	9.8
75-150	17.1	56.0	42.7[c]	8.5

[abc] Means without common superscript differ at $p < 0.01$

Summary statistics for percent gypsum are presented in Table 7. Levels of gypsum increase from the first to the second depth, and then a decrease occurs from the second to third depth. This may be the result of shale occurring at shallow depths in some cores, and field observations suggested that the shale contained less gypsum than the lower solum.

Table 7. Summary statistics for gypsum content.

Depth	Gypsum Concentration			
	Minimum	Maximum	Mean	Standard
cm	%			Deviation
0-25	0.0	26.6	2.0[ac]	6.2
25-75	0.0	29.2	8.5[bd]	8.4
75-150	0.3	18.6	5.5[abe]	4.9

[ab] Means without common superscript differ at $p < 0.01$.
[cde] Means without common superscript differ at ($p < 0.1$)

Classical Statistical Analyses

Classical statistics were used to relate apparent EC to the laboratory analyses for each depth of sampling. Table 8 gives the r^2 value for the Pearson's Partial Correlation (SAS, 1999). All correlations in Table 8 were based on 29 observations. The number in parentheses (1,2, or 3) behind the variable in column one indicates the depth zone with number 1 representing samples from 0 to 25 cm, number 2 from 25 to 75 cm, and number 3 from 75 to 150 cm.

The moisture content shows no correlation to apparent EC in July (Table 8), and only a moderate correlation to apparent EC in November for the first two depths. It is believed that this correlation would have been stronger if volumetric water content had been measured instead of gravimetric water content. Table 4 (Tables on p. 65 and 68) also shows that the overall range of moisture content in November was higher than in July. This remained true for the mean readings as the mean percent moisture in July was 18.8% and in November, it increased to 24.8%.

As expected, there is a significant correlation between EC of the saturated paste extract and apparent EC measurements. Readings were taken in the vertical dipole mode, and previous research has shown that the influence of the apparent EC would be mainly from soil properties found between 25 to 75 cm. Statistical results for this research support this, as EC in the second and third depths are more significantly correlated to apparent EC. The EC of the

saturated paste measurements had a minimum value of 0.5 dS m^{-1}, a maximum value of 6.3 dS m^{-1}, and a mean of 3.0 dS m^{-1} (found in Table B-4 of Appendix B). When the apparent EC was correlated to EC of the saturated paste extract, a r^2 value of 0.32 ($p < 0.05$) for the second depth zone (25-75 cm) and 0.51 for the third depth zone (75-150 cm) was calculated for July. The correlated between apparent EC in November and EC of the saturated paste extract had a r^2 value of 0.16 and 0.15 ($p < 0.05$) for the second and third depth zones, respectively.

Table 8. Correlation of apparent EC in July and November with selected soil properties at three depths.

Variable and Depth	Apparent EC July mS m^{-1} (r^2, p)	Apparent EC November mS m^{-1} (r^2, p)
EC (1), dS m^{-1}	0.05, 0.25	0.05, 0.22
EC (2), dS m^{-1}	0.32, <0.01	0.16, 0.03
EC (3), dS m^{-1}	0.51, <0.01	0.15, 0.03
SO_4^{2-} (1), mmol (-) L^{-1}	0.05, 0.25	0.05, 0.26
SO_4^{2-} (2), mmol (-) L^{-1}	0.30, <0.01	0.16, 0.03
SO_4^{2-} (3), mmol (-) L^{-1}	0.11, 0.08	0.03, 0.35
Percent Moisture (1) Oven Dried	0.00, 0.89	0.26, <0.01
Percent Moisture (2) Oven Dried	0.00, 0.97	0.17, 0.02
Percent Moisture (3) Oven Dried	0.01, 0.64	0.05, 0.79
Percent Gypsum (1)	0.01, 0.68	0.02, 0.52
Percent Gypsum (2)	0.06, 0.19	0.03, 0.34
Percent Gypsum (3)	0.15, 0.04	0.28, <0.01

*1,2, or 3 following a variable in the first column indicates sampling depth zone. 1 = 0-25 cm, 2 = 25-75 cm, and 3 = 75-150 cm.

To determine if the EM38 is a good device for detecting sulfate mineral, the correlation between sulfate and apparent EC was considered, as well as percent gypsum. Although there were slight significant correlations between these variables, correlation coefficients were low. For July, the only significant correlation between sulfate and apparent EC was found in the second depth zone (25-75 cm) where the r^2 value was 0.30. Percent gypsum produced a similar correlation (r^2 = 0.15) with July apparent EC, except that the significant correlation was in the third depth zone (75-150 cm). Similarly, the soluble SO_4^{2-} is most highly correlated in the 25-75 cm zone in November, although the correlation is weaker than in the July data (Table 8).

Two other important relationships to understand (Table 9) are between SO_4^{2-} and EC of the saturated paste extract, and Cl^- and EC of the saturated paste extract. For the relationship between SO_4^{2-} and EC of the saturated paste extract, significant correlations are found at all depths. Sulfate and EC in the first depth zone gives a r^2 value of 0.91, and in the second depth zone a r^2 = 0.73. The correlation was still significant in the third depth zone, but was considerably weaker (r^2 = 0.16). To confirm that SO_4^{2-} is the primary source contributing to EC of the saturated paste extract, the relationship between Cl^- and EC of the saturated paste extract was examined. No significant correlations were found at any of the three depth zones and r^2 values at each depth were extremely low (first depth zone r^2 = 0.08, second depth zone r^2 = 0.01, third

depth zone r^2 = 0.12) confirming that SO_4^{2-} is the anion most responsible for the EC of the saturated paste extract.

Table 9. Correlation matrix of EC of the saturated paste extract with SO_4^{2-} and Cl^-.

	EC dS m^{-1} (r^2, p)
SO_4^{2-} (1), mmol (-) L^{-1}	0.91, <0.01
SO_4^{2-} (2), mmol (-) L^{-1}	0.73, <0.01
SO_4^{2-} (3), mmol (-) L^{-1}	0.16, 0.03
Cl^- (1), mmol (-) L^{-1}	0.08, 0.13
Cl^- (2), mmol (-) L^{-1}	0.01, 0.59
Cl^- (3), mmol (-) L^{-1}	0.12, 0.06

Results from the classical statistical analyses suggest that to quantify soluble salts using the EM38, moisture influence should be minimized. This can be done by sampling in the drier months when moisture content is considerably lower and does not influence the apparent EC as much. This is contrary to what previous research suggests, that is, measurements should be taken when the soil profile is near field capacity in order to eliminate variable water contents as a factor affecting apparent EC measurements (Rhoades and Ingvalson, 1971). Statistics also show that the EM38 successfully detects changes in apparent EC

at the deeper depths measured by the vertical dipole orientation. Relationships between the apparent EC and sulfate and percent gypsum exist, but are weak. Finally, a strong relationship exists between EC of the saturated paste extract and soluble sulfate in this study area, especially in the upper two sampling depths.

Spatial Statistical Analyses

In addition to the spatial statistics previously presented for the apparent EC values, regression kriging was done for EC of the saturated paste extract because of the significant relationship between EC of the saturated paste extract and apparent EC measurements. Regression kriging allowed for predictions of EC of the saturated paste extract to be made using both 1) the spatial structure of the apparent EC data, and 2) the relationship between apparent EC and EC of the saturated paste extract.

The EC of the saturated paste extract was predicted on a regularly spaced grid across the field using regression kriging. This necessitated the development of an equation relating apparent EC to the EC of the saturated paste extract. Figure 11 gives the equation used for the regression kriging for the second depth of EC of the saturated paste extract and apparent EC in July.

Figure 12 is the kriged map of EC of the saturated paste extract in the second depth zone (25-75 cm) as predicted from the apparent EC measurements in July. Predicted EC of the saturated paste extract in the second depth zone ranged from 1.05 to 2.05 dS m^{-1}. A range of 0.7 to 3.7

dS m^{-1} was found for the raw data of the EC of the saturated paste extract (Table B-4). This difference in range is a result of smoothing by the simple linear model shown in Fig. 11. Trends for the study area are similar to those found with the apparent EC kriged map (Fig. 9). Values tend to be lowest in the southeast corner of the plot and increase downslope towards the northwest. Concentrations of high EC values can also be found along the west boundary of the field.

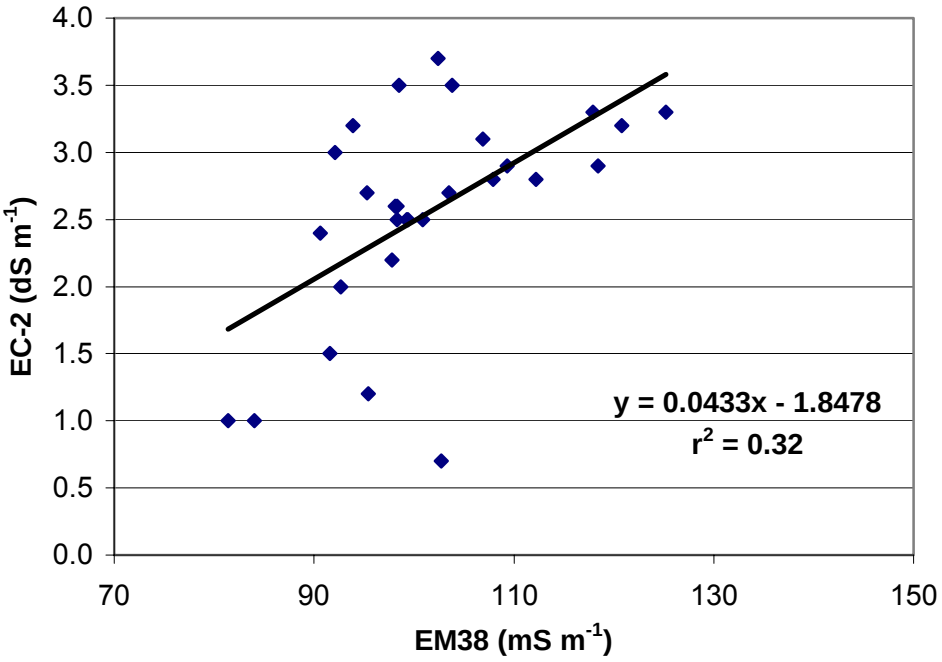

Fig. 11. Simple linear model used for regression kriging performed on the second depth zone (25-75 cm).

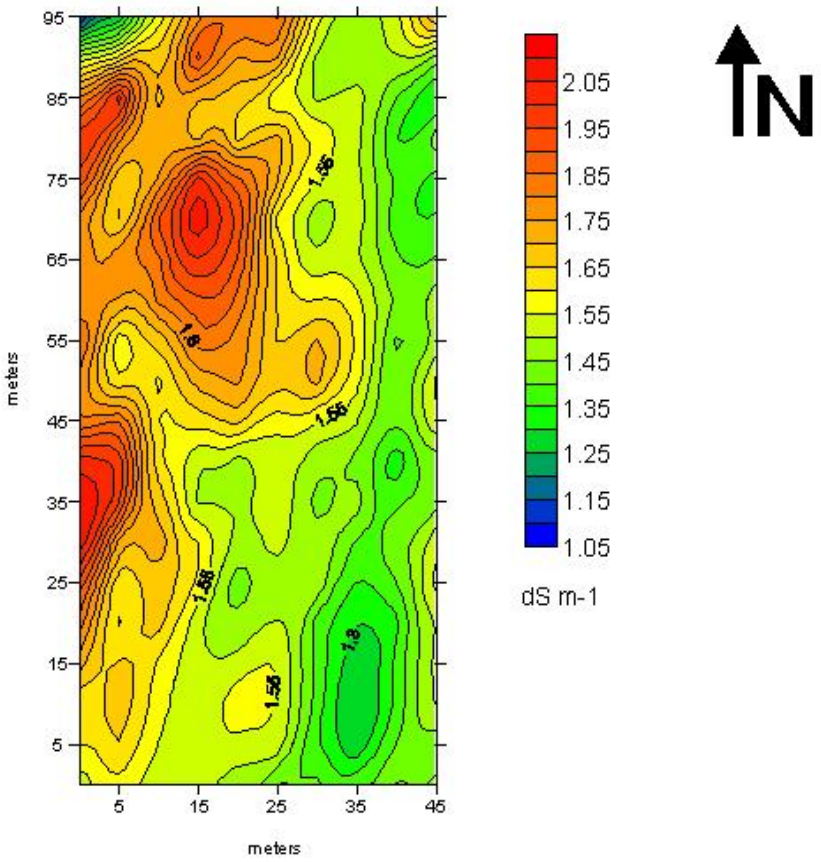

Fig. 12. Electrical conductivity of the saturated paste extract in the second depth zone as predicted from apparent EC in July using regression kriging.

Figure 13 shows the simple linear model used to perform regression kriging of EC of the saturated paste extract in the third depth zone, and Fig. 14 is the map showing EC of the saturated paste extract in the third depth zone (75-150 cm) kriged from apparent EC data in July. The trends are similar to those just described for EC trends in the second depth zone. The range for this map is different than the predicted EC values in the second depth zone with the minimum of the range being 4.8 dS m^{-1} and a maximum of 6.0 dS m^{-1}, while the range for the raw data of EC of the saturated paste extract (Table B-4) is 4.2 to 6.3 dS m^{-1}. This similarity of ranges in the third depth zone, but not in the second, was because less smoothing of the linear model occurred since EC of the saturated paste extract and apparent EC in the third depth zone were more highly correlated.

Regression kriging allows values of a selected variable to be predicted at high spatial resolution across a field using a small number of soil core observations collected at a relatively low spatial resolution. The accuracy of regression kriging is dependant on (1) strength of the spatial structure of the high resolution data, apparent EC in this case, and (2) the strength of the correlation between the high resolution and low spatial resolution data (apparent EC and EC of the saturated paste extract). The effect of a stronger versus weaker correlation between the two variables was illustrated by the results of the second depth zone and the third depth zone.

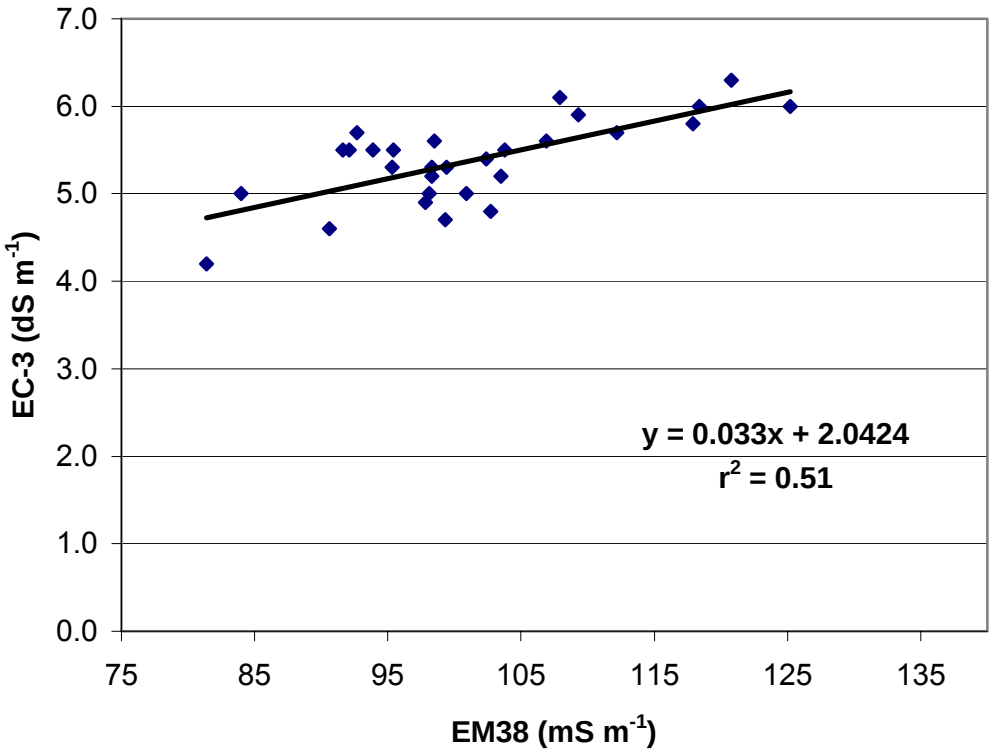

Fig. 13. Simple linear model used for regression kriging performed on the third depth zone (75-150 cm).

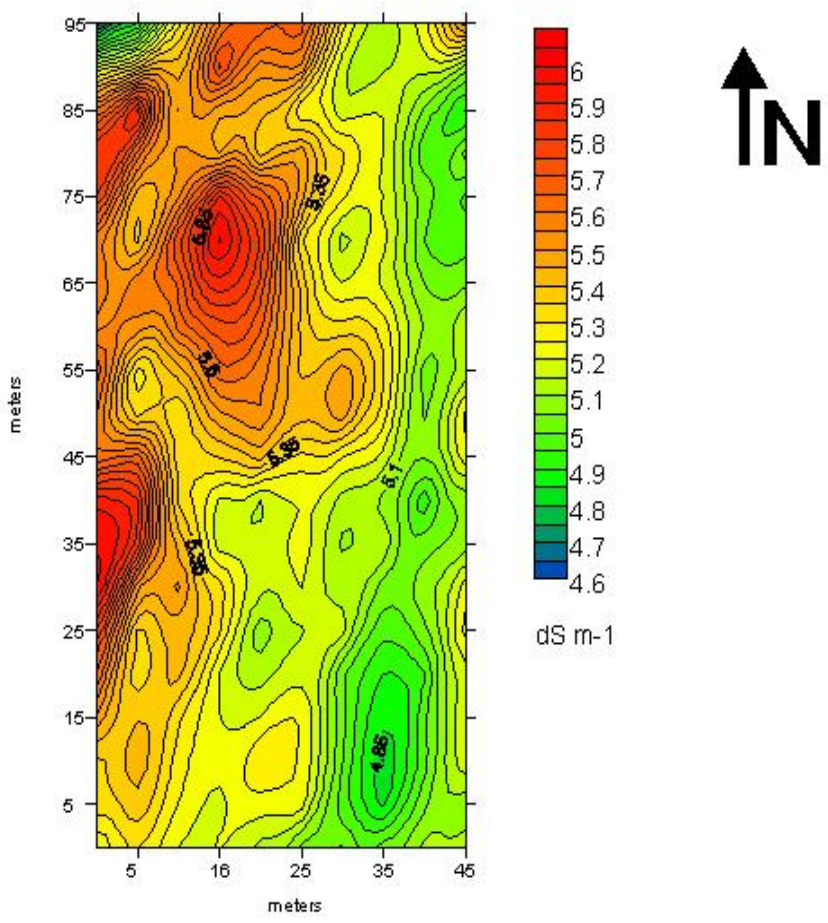

Fig. 14. Electrical conductivity of the saturated paste extract in the third depth zone as predicted from apparent EC in July using regression kriging.

CONCLUSIONS

The first objective of this research was to document variability of EC within a selected site containing sulfate-bearing minerals. This was successfully completed using the EM38 instrument. As results showed, there is a significant correlation between the apparent EC using the EM38 in the vertical dipole orientation and EC of the saturated paste extract at the deeper depths. Approximately 51% of the variability in the apparent EC data was explained by the EC in the deepest zone (75-150 cm) when measured when the soil was relatively dry (July).

Using the data collected in the field, it was possible to calculate semivariance and produce a semivariogram to determine the extent of spatial correlation within the plot of the apparent EC. Values were kriged and maps showing predicted EC values for the field were generated, enabling an estimation of values in areas that were not sampled in a time and cost efficient manner.

Predicting apparent EC using the EM38 can be successfully done again in different areas, but it must be emphasized that core samples must be taken in every field to determine baseline values for each particular area. In other words, data cannot be extrapolated from one field to the next. This is a disadvantage of using a unit such as the EM38, but overall, costs of the EM38 are fixed, and using the EM38 over large areas may save time.

The second objective for this research was to determine if electromagnetic induction is an efficient technique for locating high levels of sulfate-bearing minerals using data from the first objective. Results suggest that it may not be adequate.

It was obvious that apparent EC values are a reflection of several variables in the soil, and their influence needed to be minimized in order to detect sulfate levels. Influences of clay content and type were not a concern, as the research plot was considered uniform in this respect. Moisture content influenced the apparent EC values, as range and mean readings were higher in November than in July when the soil was drier. Correlations of soluble sulfate, EC of the saturated paste extract, and gypsum percentage to apparent EC were higher for the July data set than in November. Because of the need to reduce the influence of moisture on apparent EC to allow greater sensitivity to soluble salts, it was concluded that sampling during periods of low soil moisture content would be better.

Classical statistical analyses showed that there was a relationship between sulfate in the second depth zone and apparent EC in July ($r^2 = 0.30$) as well as percent gypsum in the third depth zone ($r^2 = 0.15$). Although sulfate and gypsum were significantly correlated with EM38 readings, correlations were weak and apparent EC would not serve as a good quantifier of sulfate-bearing materials.

For future research in this area, some suggestions can be made. First, multiple sites for conducting the survey should be used. Sites should have a wide range in the concentration of soluble sulfate, including none, moderate, and high levels of sulfate-bearing materials. Second, previous research has indicated surveys should be conducted when the soil is near field capacity in order to minimize variations in the effect soil moisture content has on apparent EC. Field capacity should also allow the electrical current to flow continuously throughout the profile instead of encountering interruptions that may occur in conditions drier than field capacity. Studies at the higher moisture level (near field capacity) should be compared to results at low moisture contents to test the validity of the findings of this study. Finally, when dividing soil cores into sampling depth intervals, it is suggested that the intervals include a zone where the sensitivity of the instrument is at a maximum (40-75 cm). Incorporating these suggestions would allow for questions associated with this research to be absolved.

REFERENCES

Amethyst Galleries, Inc. 1996. The Mineral Ettringite. [Online]. http://mineral.galleries.com/minerals/sulfates/ettringi/ettringi.htm

Burgess, T.M., and R. Webster. 1980. Optimal interpolation and isarithmic mapping of soil properties, the semivariogram and punctual kriging. J. Soil Sci. 31: 315-331.

Cressie N.A.C. 1993. Statistics for Spatial Data. Revised Edition. Wiley, New York.

Davis, J.G., N.R. Kitchen, K.A. Sudduth, and S.T. Drummond. 1997. Using Electromagnetic Induction to Characterize Soils. Better Crops with Food. No. 4. Potash and Phosphate Institute. Norcross, GA.

Doerge, T.A., N.R. Kitchen, and E.D. Lung. 2003. Site Specific Management Guidelines #30, Soil Electrical Conductivity Mapping. Potash and Phosphate Institute. Norcross, GA.

Doolittle, J.A., S.J. Indorante, D.K. Potter, S.G. Hefner, and W.M. McCauley. 2002. Comparing three geophysical tools for locating sand blows in alluvial soils of southeast Missouri. J. Soil Water Conserv. 57:175-182.

Fanning, D.S., M.C. Rabenhorst, S.N. Burch, K.R. Islam, and S.A. Tangren. 2002. Sulfides and sulfates. pp. 229-260. *In* J.B. Dixon and D.G. Schulze (eds.) Soil Mineralogy with Environmental Applications. Soil Science Society of America Book Series (7). Soil Sci. Soc. Am., Inc., Madison, WI.

Geonics Limited. 2002. EM38B Ground Conductivity Meter Dual Output Version Operating Manual. Mississauga, Ontario.

Hallmark, C.T. 1993. The nature and origin of blackland soils. pp. 42-47. *In* M.R. Sharpless and J.C. Yelderman, Jr (eds.) The Texas Blackland Prairie, Land, History, and Culture. Waco, TX.

Hallmark, C.T., L.T. West, L.P. Wilding, and L.R. Drees. 1986. Characterization Data for Selected Texas Soils. Texas Agric. Exp. Stn. MP-1583. Texas A&M University, College Station, TX.

Huckabee, J.W., D.R. Thompson, J.C. Wyrick, and E.G. Pavlat. 1977. Soil Survey of Bell County, Texas. USDA, NRCS, U.S. Government Printing, Washington, DC.

Hunter, D. 1988. Lime induced heave in sulfate-bearing clay soils. ASCE. J. Geotech. Eng. 114:150-167.

Jackson, M.L. 1958. Soil Chemical Analysis. Prentice-Hall, Engle Cliffs, NJ.

Jurinak, J.J. 1990. The chemistry of salt-effected soils and water. pp.42-63. *In* K.K. Tanja (ed.) Agricultural Salinity Assessment and Management. American Society of Civil Engineers, New York.

Little, D.N. 2000. Evaluation of structural properties of lime stabilized soils and aggregates. Volume 3. [Online]. www.lime.org/soil3.pdf

McNeill, J.D. 1980. Electromagnetic terrain conductivity measurement at low induction numbers. Technical Note TN-6. Geonics Limited, Ontario, Canada.

Merrill, B.D. 1998. Durability of Concrete in Highway Facilities. University of Houston. Houston, TX.

Mulla, D.J. 1989. Soil spatial variability and methods of analysis. International Crops Research Institute for Semi-Arid Tropics. Proc. for an International Workshop. 7-11 Jan. 1987 *In* Soil Sci. Soc. Am., Inc., Madison, WI.

Nielsen, D.R., and O. Wendroth. 2003. Spatial and Temporal Statistics, Sampling Field Soils and Their Vegetation. Catena-Verlag GMBH, Reiskirchen, Germany.

Powrie, W. 1997. Soil Mechanics Concepts and Applications. 1st Ed. E and FN Spon, London, UK.

Rhoades, J.D. and R.D. Ingvalson. 1971. Determining salinity in field soils with soil resistance measurements. Soil Sci. Soc. Am. Proc. 35:54-60.

Rhoades, J.D., P.A.C. Ratts, and R.J. Prather. 1976. Effects of liquid-phase electrical conductivity, water content, and surface conductivity on bulk soil electrical conductivity. Soil Sci. Soc. Am. J. 40:651-655.

Sabry, M.A., L.W. Reed, and J.V. Parcher. 1981. Mineralogy of compacted clay-lime mixtures. Soil Sci. Soc. Am. J. 45:144-150.

SAS Institute, Inc. 1999. SAS User's Guide: Statistics. Release 8.1, SAS Institute, Inc. Cary, NC.

Sherwood, P.T. 1993. Soil stabilization with cement and lime. State of the Art Review, HMSO, London.

Soil Survey Laboratory Staff. 1996. Soil Survey Laboratory Methods Manual. Soil Investigations Report No. 42. Version 3.0. USDA, NRCS, Lincoln, NE.

Soil Survey Laboratory Staff. 1972. Soil survey laboratory methods and procedures for collecting soil samples. Soil Survey Investigations Report No.1. USDA, NRCS, U.S. Government Printing, Washington, DC.

S-Plus 6.0 Professional for Windows. 2001. S-Plus User's Guide. Release 2. Insightful Corporation, Lucent Technologies, Inc. Seattle, WA.

Stark, J., and K. Bollmann. 1998. Delayed Ettringite Formation in Concrete. Nordic Concrete Federation. Weimar,Germany.

Surfer 8. 2002. Surfer 8 User's Guide. Golden Software, Inc. Golden, CO.

Texas Transportation Institute. 2003. Exploding Roads. Texas Transportation Research Vol. 39 No. 1. Texas Transportation Institution, College Station, TX.

Upchurch, D.R., and W.J. Edmonds. 1991. Statistical procedures for specific objectives. pp. 49-71. *In* M.J.Mausbach and L.P. Wilding (eds.) Spatial Variabilities of Soils and Landforms. Soil Science Society of America Special Publication Number 28. Soil Sci. Soc. Am., Inc., Madison, WI.

US Department of Transportation-Federal Highway Administration. 2002. Guidelines for Detection, Analysis, and Treatment of Materials-Related Distress in Concrete Pavements. [Online]. http://www.tfhrc.gov/pavement/pubs/01163.

APPENDIX A

20	72.7	81.4*	98.3	107.9	111.4	112.9	97.7	91.7	96.0	110.9
19	97.7	98.3*	101.3	117.8	105.2	108.9	94.1	93.9	94.6	90.0
18	109.1	125.2*	101.7	102.7	102.7	94.4	93.2	96.2	90.2	83.3
17	117.7	107.9*	106.2	100.4	97.9	107.1	100.1	96.1	87.1	94.1
16	116.6	100.9*	105.6	122.2	112.0	105.0	98.2	96.3	90.5	86.3
15	106.4	99.4*	114.4	123.4	115.4	96.4	91.7	97.6	88.6	88.2
14	109.5	109.3*	108.8	117.7	113.7	102.2	95.2	94.9	90.7	90.4
13	104.6	106.9*	110.1	112.4	110.7	101.4	99.2	98.3	92.7	95.2
12	113.3	95.3*	102.4	110.7	107.5	100.8	105.3	99.2	88.8	93.1
11	108.6	98.1*	97.3	105.3	107.8	103.1	106.5	99.1	89.9	99.4
10	106.9	112.2*	98.2	100.7	104.3	97.7	96.4	95.9	91.3	98.3
9	120.8*	118.4*	98.5*	93.9*	92.1*	95.4*	92.7*	91.6*	84.0*	90.6*
8	120.5	117.9*	103.8	93.1	94.9	97.4	91.4	95.7	90.3	90.5
7	123.5	103.5*	107.8	100.6	94.6	96.7	93.2	89.5	93.1	97.5
6	114.7	98.3*	103.0	99.8	90.1	93.6	96.4	87.9	90.5	99.1
5	110.9	97.8*	103.6	95.0	93.3	95.1	88.1	85.7	86.3	94.7
4	105.5	102.4*	98.6	95.8	95.4	97.9	90.0	84.5	89.5	96.3
3	98.9	103.8*	97.9	96.3	100.1	97.2	89.5	83.3	88.3	96.0
2	100.1	102.7*	97.2	94.5	96.3	98.3	88.0	82.5	90.4	90.3
1	94.3	99.3*	95.3	96.3	93.0	88.9	92.3	90.5	93.6	93.4
	1	**2**	**3**	**4**	**5**	**6**	**7**	**8**	**9**	**10**

N

*Indicates points where cores were taken.

Fig. A-1. EM38 readings (mS m^{-1}) taken on July 22, 2003.

20	125.9	145.7 *	139.2	148.0	145.5	147.2	125.7	115.4	125.7	135.8
19	152.3	155.3 *	149.7	151.2	131.2	140.0	122.9	121.7	117.1	113.8
18	161.8	167.3 *	140.1	133.4	136.9	122.8	125.7	121.3	112.9	109.8
17	164.9	156.2 *	151.6	136.9	131.2	138.9	136.3	124.1	122.8	125.9
16	159.2	144.3 *	144.6	158.7	154.3	134.5	125.2	126.2	115.7	118.6
15	158.9	140.3 *	153.4	156.7	155.6	135.6	124.3	128.5	115.7	114.8
14	155.2	148.6 *	146.5	153.5	152.1	141.5	125.7	127.9	118.1	116.4
13	147.4	142.2 *	143.2	154.1	151.2	140.3	135.0	133.5	120.2	116.0
12	149.7	134.3 *	142.6	152.3	151.6	145.2	141.3	141.5	122.6	116.4
11	149.4	135.6 *	133.6	145.9	147.2	142.9	145.5	138.3	126.8	123.4
10	153.9	148.6 *	136.5	144.2	142.1	140.5	116.9	118.4	118.9	128.6
9	158.7 *	154.5 *	138.5 *	131.2 *	126.7 *	122.0 *	117.8 *	120.8 *	113.0 *	117.7 *
8	163.1	153.0 *	146.9	125.8	124.5	123.2	122.0	115.4	108.9	108.9
7	161.2	144.3 *	147.4	131.5	126.3	134.4	137.1	121.3	115.4	120.5
6	155.5	142.1 *	139.3	137.2	128.3	135.7	138.9	119.8	111.3	120.1
5	154.1	137.3 *	143.3	133.2	129.9	132.4	125.1	106.9	105.8	120.7
4	140.2	133.4 *	139.8	131.8	133.3	134.7	130.1	111.7	112.9	125.0
3	134.1	145.6 *	139.5	134.2	137.1	134.3	120.7	107.9	115.4	117.7
2	136.0	149.1 *	136.8	132.7	134.3	130.2	122.9	115.7	116.7	122.4
1	137.6	137.4 *	143.6	142.5	135.8	123.4	126.4	117.8	128.2	136.0
	1	**2**	**3**	**4**	**5**	**6**	**7**	**8**	**9**	**10**

N

*Indicates points where cores were taken.

Fig. A-2. EM-38 readings (mS m^{-1}) taken on November 13, 2003.

Table A-1. Additional EM38 readings for November 13, 2003.

Observation column_row_interval	EM38 Reading mS m^{-1}	Observation column_row_interval	EM38 Reading mS m^{-1}
1_9_0	158.7	7_9_33	116.7
1_9_1	158.3	7_9_34	122.3
1_9_2	154.8	8_9_35	120.8
1_9_3	155.8	8_9_36	122.9
1_9_4	156.2	8_9_37	117.7
2_9_5	154.4	8_9_38	115.2
2_9_6	149.9	8_9_39	107.3
2_9_7	145.3	9_9_40	114.6
2_9_8	142.2	9_9_41	109.4
2_9_9	139.5	9_9_42	111.7
3_9_10	137.9	9_9_43	117.2
3_9_11	134.0	9_9_44	120.4
3_9_12	129.3	10_9_45	117.7
3_9_13	133.1	4_1_0	142.5
3_9_14	125.6	4_1_1	136.9
4_9_15	129.8	4_1_2	133.3
4_9_16	127.4	4_1_3	131.5
4_9_17	125.3	4_1_4	128.4
4_9_18	125.2	4_2_5	132.3
4_9_19	127.2	4_2_6	129.5
5_9_20	127.0	4_2_7	135.9
5_9_21	129.4	4_2_8	136.9
5_9_22	127.4	4_2_9	134.5
5_9_23	127.8	4_3_10	136.1
5_9_24	130.1	4_3_11	138.2
6_9_25	122.7	4_3_12	131.1
6_9_26	127.3	4_3_13	133.3
6_9_27	127.3	4_3_14	139.0
6_9_28	119.7	4_4_15	131.8
6_9_29	120.5	4_4_16	128.8
7_9_30	114.9	4_4_17	128.1
7_9_31	116.8	4_4_18	133.3
7_9_32	116.1	4_4_19	128.6

Table A-1. Continued.

Observation	EM38 Reading
column_row_interval	mS m^{-1}
4_5_20	128.8
4_5_21	136.0
4_5_22	129.9
4_5_23	130.4
4_5_24	128.4
4_6_25	127.6
4_6_26	131.6
4_6_27	126.8
4_6_28	126.2
4_6_29	123.4
4_7_30	125.7
4_7_31	120.7
4_7_32	125.5
4_7_33	127.4
4_7_34	131.5
4_8_35	125.7
4_8_36	124.4
4_8_37	129.3
4_8_38	125.2
4_8_39	128.8
4_9_40	126.6
4_9_41	128.4
4_9_42	132.5
4_9_43	129.2
4_9_44	135.5
4_10_45	139.2

APPENDIX B

Table B-1. Moisture content of soil cores taken in July, 2003.

Observation column_row_depth	Moist Weight g	Air Dried Weight g	Air Dried Percent Moisture	Moisture Factor	Oven Dried Percent Moisture
2_1_1	1179.92	1154.92	2.2	1.079	10.1
2_1_2	2329.92	2144.92	8.6	1.078	16.4
2_1_3	4609.92	4019.92	14.7	1.079	22.6
2_2_1	1161.92	1090.42	6.6	1.086	15.2
2_2_2	2674.92	2344.92	14.1	1.082	22.3
2_2_3	4791.92	4084.92	17.3	1.065	23.8
2_3_1	1061.92	977.92	8.6	1.091	17.7
2_3_2	3471.92	3106.92	11.7	1.072	18.9
2_3_3	2040.92	1761.92	15.8	1.067	22.5
2_4_1	512.92	476.92	7.5	1.078	15.3
2_4_2	1778.92	1594.92	11.5	1.076	19.1
2_4_3	1695.92	1617.92	4.8	1.058	10.6
2_5_1	535.53	494.92	8.2	1.090	17.2
2_5_2	1088.92	1080.92	0.7	1.099	10.6
2_5_3	1817.92	1622.92	12.0	1.067	18.7
2_6_1	479.94	450.42	6.6	1.085	15.1
2_6_2	1085.92	1006.83	7.9	1.088	16.7
2_6_3	1904.46	1654.59	15.1	1.068	21.9
2_7_1	601.92	558.70	7.7	1.113	19.0
2_7_2	1260.11	1152.05	9.4	1.112	20.6
2_7_3	1928.92	1676.63	15.0	1.068	21.8
2_8_1	438.92	415.74	5.6	1.088	14.4
2_8_2	1137.92	1056.53	7.7	1.069	14.6
2_8_3	1588.92	1538.66	3.3	1.070	10.3
2_9_1	447.92	445.92	0.4	1.088	9.2
2_9_2	1218.92	1080.72	12.8	1.094	22.2
2_9_3	1822.92	1589.26	14.7	1.073	22.0
2_10_1	510.30	469.16	8.8	1.086	17.4
2_10_2	1033.92	922.42	12.1	1.095	21.6
2_10_3	1801.92	1563.92	15.2	1.082	23.4
2_11_1	659.92	641.25	2.9	1.083	11.2
2_11_2	738.07	656.75	12.4	1.091	21.5
2_11_3	1823.47	1556.20	17.2	1.081	25.3
2_12_1	390.67	356.47	9.6	1.080	17.6
2_12_2	957.22	842.92	13.6	1.110	24.6
2_12_3	1819.92	1594.44	14.1	1.078	21.9

Table B-1. Continued.

Observation column_row_depth	Moist Weight g	Air Dried Weight g	Air Dried Percent Moisture	Moisture Factor	Oven Dried Percent Moisture
2_13_1	453.32	416.36	8.9	1.083	17.2
2_13_2	1153.53	1042.28	10.7	1.088	19.5
2_13_3	1757.92	1565.78	12.3	1.081	20.4
2_14_1	409.16	375.15	9.1	1.086	17.7
2_14_2	1022.34	940.93	8.7	1.090	17.7
2_14_3	1708.57	1563.06	9.3	1.077	17.0
2_15_1	528.06	486.60	8.5	1.083	16.8
2_15_2	1165.60	1047.30	11.3	1.086	19.9
2_15_3	1801.49	1493.26	20.6	1.071	27.7
2_16_1	417.09	375.67	11.0	1.077	18.7
2_16_2	1158.75	1020.97	13.5	1.086	22.1
2_16_3	1788.20	1520.97	17.6	1.076	25.2
2_17_1	614.01	558.31	10.0	1.109	20.9
2_17_2	1096.48	966.04	13.5	1.106	24.1
2_17_3	1887.34	1581.56	19.3	1.074	26.7
2_18_1	458.07	419.79	9.1	1.087	17.8
2_18_2	994.77	970.08	2.5	1.097	12.2
2_18_3	1833.97	1537.82	19.3	1.075	26.8
2_19_1	527.50	485.42	8.7	1.084	17.1
2_19_2	969.72	914.28	6.1	1.094	15.5
2_19_3	1855.45	1562.35	18.8	1.080	26.8
2_20_1	483.05	443.69	8.9	1.086	17.5
2_20_2	1040.52	942.94	10.3	1.085	18.8
2_20_3	1825.92	1633.50	11.8	1.078	19.6
1_9_1	503.55	455.83	10.5	1.085	19.0
1_9_2	1123.92	1084.89	3.6	1.095	13.1
1_9_3	1868.92	1570.01	19.0	1.069	25.9
3_9_1	508.62	472.26	7.7	1.079	15.6
3_9_2	1127.24	1005.46	12.1	1.077	19.8
3_9_3	1880.02	1608.28	16.9	1.078	24.7
4_9_1	440.65	399.30	10.4	1.078	18.2
4_9_2	1142.92	1012.66	12.9	1.080	20.9
4_9_3	1765.92	1546.71	14.2	1.079	22.1
5_9_1	551.91	501.65	10.0	1.080	18.0
5_9_2	1008.72	936.51	7.7	1.090	16.7
5_9_3	1840.86	1580.27	16.5	1.086	25.1
6_9_1	362.62	353.50	2.6	1.082	10.8
6_9_2	981.96	978.71	0.3	1.078	8.1

Table B-1. Continued.

Observation column_row_depth	Moist Weight g	Air Dried Weight g	Air Dried Percent Moisture	Moisture Factor	Oven Dried Percent Moisture
6_9_3	1760.12	1578.67	11.5	1.081	19.6
7_9_1	558.72	538.11	3.8	1.081	11.9
7_9_2	949.77	914.04	3.9	1.082	12.1
7_9_3	1797.60	1585.59	13.4	1.080	21.4
8_9_1	518.42	477.64	8.5	1.081	16.6
8_9_2	1133.31	1023.59	10.7	1.081	18.8
8_9_3	1896.23	1629.84	16.3	1.081	24.4
9_9_1	453.02	416.90	8.7	1.077	16.4
9_9_2	947.12	894.14	5.9	1.081	14.0
9_9_3	1859.22	1656.65	12.2	1.093	21.5
10_9_1	476.58	440.34	8.2	1.094	17.6
10_9_2	1089.92	1029.39	5.9	1.117	17.6
10_9_3	1914.32	1661.38	15.2	1.096	24.8
Minimum	362.62	353.50	0.3	1.06	8.1
Maximum	4791.92	4084.92	20.6	1.11	27.7
Mean	1285.27	1149.67	10.4	1.08	18.8
Standard Deviation	817.28	700.74	4.7	0.01	4.5

Table B-2. Moisture content of soil cores taken in November, 2003.

Observation column_row_depth	Moist Weight g	Air Dried Weight g	Air Dried Percent Moisture	Moisture Factor	Oven Dried Percent Moisture
2_1_1	438.16	373.70	17.25	1.045	21.7
2_1_2	1210.74	998.41	21.27	1.046	25.9
2_1_3	1973.56	1671.26	18.09	1.067	24.8
2_2_1	470.64	402.00	17.07	1.047	21.8
2_2_2	1109.00	923.88	20.04	1.046	24.6
2_2_3	1904.85	1590.27	19.78	1.041	23.8
2_3_1	544.60	458.73	18.72	1.047	23.4
2_3_2	1117.09	916.46	21.89	1.048	26.7
2_3_3	1891.58	1590.64	18.92	1.054	24.3
2_4_1	436.41	378.54	15.29	1.049	20.2
2_4_2	1098.55	928.27	18.34	1.045	22.9
2_4_3	1734.69	1474.76	17.63	1.051	22.7
2_5_1	524.07	443.51	18.16	1.044	22.6
2_5_2	1077.25	863.53	24.75	1.048	29.5
2_5_3	1873.13	1605.44	16.67	1.118	28.4
2_6_1	489.48	415.73	17.74	1.047	22.5
2_6_2	1143.83	940.31	21.64	1.084	30.0
2_6_3	1870.01	1544.39	21.08	1.051	26.2
2_7_1	441.59	369.78	19.42	1.049	24.4
2_7_2	1188.53	975.16	21.88	1.048	26.7
2_7_3	1798.58	1536.70	17.04	1.082	25.2
2_8_1	491.64	430.63	14.17	1.104	24.6
2_8_2	1144.38	1015.15	12.73	1.105	23.2
2_8_3	1831.36	1550.52	18.11	1.070	25.1
2_9_1	499.21	419.97	18.87	1.048	23.7
2_9_2	1140.53	948.27	20.27	1.076	27.8
2_9_3	1823.13	1495.82	21.88	1.041	26.0
2_10_1	443.23	381.75	16.10	1.049	21.0
2_10_2	1126.65	966.36	16.59	1.081	24.7
2_10_3	1812.90	1481.53	22.37	1.042	26.6
2_11_1	512.22	434.16	17.98	1.056	23.6
2_11_2	1131.44	930.47	21.60	1.054	27.0
2_11_3	1834.95	1502.33	22.14	1.053	27.5
2_12_1	513.53	447.27	14.81	1.057	20.5
2_12_2	1181.15	1038.00	13.79	1.096	23.4
2_12_3	1822.23	1538.13	18.47	1.076	26.1
2_13_1	491.03	415.47	18.19	1.056	23.8
2_13_2	1139.47	959.78	18.72	1.052	23.9

Table B-2. Continued.

Observation column_row_depth	Moist Weight g	Air Dried Weight g	Air Dried Percent Moisture	Moisture Factor	Oven Dried Percent Moisture
2_13_3	1807.31	1484.32	21.76	1.053	27.1
2_14_1	489.75	412.37	18.76	1.055	24.3
2_14_2	1142.77	931.67	22.66	1.058	28.5
2_14_3	1541.13	1245.56	23.73	1.049	28.6
2_15_1	523.67	445.42	17.57	1.048	22.4
2_15_2	1163.91	956.75	21.65	1.049	26.5
2_15_3	1893.57	1558.23	21.52	1.054	26.9
2_16_1	419.66	355.26	18.13	1.054	23.5
2_16_2	1229.97	1060.67	15.96	1.058	21.8
2_16_3	1805.09	1517.52	18.95	1.053	24.3
2_17_1	517.74	445.62	16.18	1.090	25.2
2_17_2	1307.45	1139.43	14.75	1.086	23.3
2_17_3	1853.10	1549.52	19.59	1.054	25.0
2_18_1	560.03	469.48	19.29	1.056	24.9
2_18_2	1159.25	951.72	21.81	1.064	28.2
2_18_3	1769.95	1437.58	23.12	1.046	27.7
2_19_1	561.33	474.69	18.25	1.054	23.7
2_19_2	850.62	707.73	20.19	1.051	25.2
2_19_3	1176.92	954.09	23.36	1.045	27.8
2_20_1	504.62	424.64	18.83	1.055	24.3
2_20_2	1051.62	888.77	18.32	1.050	23.3
2_20_3	1872.17	1572.00	19.09	1.044	23.5
1_9_1	496.34	424.93	16.81	1.059	22.7
1_9_2	1222.02	1014.61	20.44	1.083	28.7
1_9_3	1755.62	1437.92	22.09	1.044	26.5
3_9_1	507.76	430.62	17.91	1.050	22.9
3_9_2	1183.01	978.18	20.94	1.049	25.8
3_9_3	1905.62	1595.76	19.42	1.068	26.2
4_9_1	496.13	416.33	19.17	1.052	24.4
4_9_2	1098.98	887.07	23.89	1.051	29.0
4_9_3	1901.74	1559.21	21.97	1.041	26.1
5_9_1	509.47	431.04	18.20	1.051	23.3
5_9_2	1130.55	951.88	18.77	1.053	24.0
5_9_3	1855.17	1547.58	19.88	1.045	24.4
6_9_1	550.20	470.55	16.93	1.058	22.7
6_9_2	1124.76	924.15	21.71	1.046	26.3
6_9_3	1890.37	1566.98	20.64	1.053	25.9
7_9_1	462.00	393.86	17.30	1.060	23.3

Table B-2. Continued.

Observation column_row_depth	Moist Weight g	Air Dried Weight g	Air Dried Percent Moisture	Moisture Factor	Oven Dried Percent Moisture
7_9_2	1141.85	935.56	22.05	1.050	27.0
7_9_3	1849.47	1566.54	18.06	1.076	25.7
8_9_1	499.36	431.43	15.75	1.054	21.2
8_9_2	1119.83	949.73	17.91	1.053	23.2
8_9_3	1788.44	1469.40	21.71	1.048	26.5
9_9_1	444.98	382.78	16.25	1.051	21.4
9_9_2	1023.58	885.41	15.61	1.057	21.3
9_9_3	1853.80	1567.93	18.23	1.057	23.9
10_9_1	507.72	440.51	15.26	1.055	20.8
10_9_2	1068.04	924.86	15.48	1.058	21.3
10_9_3	1850.06	1557.08	18.82	1.074	26.2
Minimum	419.66	355.26	12.73	1.04	20.2
Maximum	1973.56	1671.26	24.75	1.12	30.0
Mean	1146.13	959.56	19.01	1.06	24.8
Standard Deviation	549.33	455.23	2.54	0.02	2.3

Table B-3. Soluble cations in the saturated paste extract of soil cores taken in July.

Observation column_row_depth	Saturated Paste Extract Ca^{2+}	Mg^{2+}	Na^{+}	K^{+}	Sum Cations
	mmol (+) L^{-1}				
2_1_1	14.0	0.7	2.0	0.1	16.8
2_1_2	26.4	1.5	7.1	0.1	35.1
2_1_3	23.0	3.3	32.2	0.2	58.7
2_2_1	3.5	0.2	1.3	0.1	5.1
2_2_2	1.5	0.2	5.3	0.0	7.0
2_2_3	23.0	3.0	32.2	0.2	58.4
2_3_1	4.4	0.3	1.6	0.1	6.4
2_3_2	24.5	2.4	20.4	0.1	47.4
2_3_3	23.0	4.0	40.4	0.2	67.6
2_4_1	12.5	1.0	2.7	0.1	16.3
2_4_2	24.5	2.5	20.9	0.1	48.0
2_4_3	24.0	4.1	39.1	0.2	67.4
2_5_1	15.5	0.6	1.7	0.1	17.9
2_5_2	25.9	1.3	5.3	0.1	32.6
2_5_3	23.5	4.1	33.0	0.2	60.8
2_6_1	26.9	1.1	2.0	0.2	30.2
2_6_2	25.9	1.6	6.9	0.1	34.5
2_6_3	24.0	4.1	33.9	0.2	62.2
2_7_1	30.9	0.6	1.3	0.1	32.9
2_7_2	27.9	2.3	6.4	0.2	36.8
2_7_3	23.0	4.9	34.3	0.3	62.5
2_8_1	8.0	0.4	1.2	0.1	9.7
2_8_2	26.9	3.0	15.7	0.2	45.8
2_8_3	23.0	5.8	43.0	0.3	72.1
2_9_1	4.4	0.3	1.0	0.1	5.8
2_9_2	26.9	2.4	13.9	0.1	43.3
2_9_3	23.0	5.8	41.7	0.3	70.8
2_10_1	4.5	0.2	0.8	0.1	5.6
2_10_2	27.4	2.2	8.3	0.2	38.1
2_10_3	23.0	4.9	39.6	0.3	67.8
2_11_1	4.2	0.2	0.9	0.1	5.4
2_11_2	26.4	2.1	7.1	0.2	35.8
2_11_3	22.0	4.9	35.7	0.3	62.9
2_12_1	25.9	0.8	0.5	0.3	27.5
2_12_2	24.5	2.8	8.4	0.3	36.0
2_12_3	22.5	6.6	38.3	0.4	67.8
2_13_1	4.4	0.3	1.2	0.1	6.0

Table B-3. Continued.

Observation column_row_depth	Saturated Paste Extract Ca^{2+}	Mg^{2+}	Na^{+}	K^{+}	Sum Cations
	mmol (+) L^{-1}				
2_13_2	26.4	2.9	13.9	0.2	43.4
2_13_3	22.5	5.8	40.4	0.3	69.0
2_14_1	9.0	0.7	1.8	0.1	11.6
2_14_2	25.9	3.0	8.9	0.2	38.0
2_14_3	22.0	5.8	42.2	0.3	70.3
2_15_1	4.4	0.3	0.9	0.2	5.8
2_15_2	26.4	2.7	5.1	0.2	34.4
2_15_3	22.0	6.6	38.3	0.3	67.2
2_16_1	6.0	0.4	0.7	0.2	7.3
2_16_2	27.9	2.5	4.8	0.2	35.4
2_16_3	22.0	6.6	35.7	0.4	64.7
2_17_1	29.4	0.8	0.9	0.2	31.3
2_17_2	25.0	3.7	11.7	0.3	40.7
2_17_3	22.0	8.2	43.5	0.4	74.1
2_18_1	27.4	2.0	1.6	0.3	31.3
2_18_2	24.5	4.9	17.4	0.3	47.1
2_18_3	22.0	7.4	45.7	0.4	75.5
2_19_1	8.5	0.6	1.5	0.3	10.9
2_19_2	28.9	2.8	3.9	0.3	35.9
2_19_3	22.5	6.6	37.4	0.4	66.9
2_20_1	6.0	0.3	1.0	0.2	7.5
2_20_2	11.0	0.7	1.7	0.1	13.5
2_20_3	23.5	4.9	25.7	0.4	54.5
1_9_1	22.0	1.2	1.4	0.2	24.8
1_9_2	26.4	3.8	16.5	0.3	47.0
1_9_3	22.5	5.8	48.7	0.4	77.4
3_9_1	3.5	0.2	1.9	0.1	5.7
3_9_2	24.5	2.6	20.9	0.2	48.2
3_9_3	23.0	4.1	41.3	0.3	68.7
4_9_1	4.5	0.4	1.5	0.1	6.5
4_9_2	25.0	2.6	17.4	0.2	45.2
4_9_3	23.0	4.9	40.4	0.3	68.6
5_9_1	4.1	0.3	1.2	0.1	5.7
5_9_2	24.5	2.1	15.2	0.2	42.0
5_9_3	24.0	4.1	40.4	0.3	68.8
6_9_1	4.2	0.3	1.8	0.1	6.4
6_9_2	3.7	0.4	12.2	0.1	16.4

Table B-3. Continued.

Observation column_row_depth	Saturated Paste Extract				
	Ca^{2+}	Mg^{2+}	Na^{+}	K^{+}	Sum Cations
	mmol (+) L^{-1}				
6_9_3	24.0	3.6	40.4	0.3	68.3
7_9_1	3.7	0.3	1.5	0.1	5.6
7_9_2	8.0	0.9	17.0	0.1	26.0
7_9_3	24.0	3.5	41.3	0.2	69.0
8_9_1	9.0	0.8	2.9	0.2	12.9
8_9_2	5.0	0.6	13.9	0.1	19.6
8_9_3	24.0	3.5	40.0	0.2	67.7
9_9_1	5.0	0.3	0.9	0.1	6.3
9_9_2	4.2	0.3	6.5	0.1	11.1
9_9_3	24.0	3.4	34.3	0.2	61.9
10_9_1	30.9	0.8	0.5	0.1	32.3
10_9_2	28.9	1.4	4.3	0.1	34.7
10_9_3	23.5	4.1	31.3	0.2	59.1
Minimum	1.5	0.2	0.5	0.0	5.1
Maximum	30.9	8.2	48.7	0.4	77.4
Mean	18.8	2.6	16.9	0.2	38.5
Standard Deviation	9.1	2.1	16.3	0.1	23.7

Table B-4. Electrical conductivity and moisture content of the saturated paste extract of the soil cores taken in July.

Observation column_row_depth	Saturated Paste Extract EC dS m^{-1}	SAR	Percent Moisture	Estimated EC* of soil solution at field moisture level dS m^{-1}
2_1_1	1.2	1	64	
2_1_2	2.5	2	54	
2_1_3	4.7	9	76	10.6
2_2_1	0.5	1	64	
2_2_2	0.7	6	70	
2_2_3	4.8	9	79	10.8
2_3_1	0.6	1	60	
2_3_2	3.5	6	67	
2_3_3	5.5	11	84	14.5
2_4_1	1.2	1	67	
2_4_2	3.7	6	65	
2_4_3	5.4	10	88	28.7
2_5_1	1.2	1	63	
2_5_2	2.2	1	59	
2_5_3	4.9	9	75	13.0
2_6_1	2.1	1	69	
2_6_2	2.6	2	66	
2_6_3	5.2	9	80	13.2
2_7_1	2.3	0	66	
2_7_2	2.7	2	61	
2_7_3	5.2	9	91	14.7
2_8_1	0.9	1	67	
2_8_2	3.3	4	71	
2_8_3	5.8	11	98	36.6
2_9_1	0.5	1	68	
2_9_2	2.9	4	70	
2_9_3	6.0	11	99	19.3
2_10_1	0.5	1	68	
2_10_2	2.8	2	66	
2_10_3	5.7	11	93	16.1
2_11_1	0.5	1	69	
2_11_2	2.6	2	69	
2_11_3	5.0	10	91	12.3
2_12_1	1.9	0	71	
2_12_2	2.7	2	62	
2_12_3	5.3	10	97	15.9

Table B-4. Continued.

Observation column_row_depth	Saturated Paste Extract EC dS m^{-1}	SAR	Percent Moisture	Estimated EC* of soil solution at field moisture level dS m^{-1}
2_13_1	0.5	1	70	
2_13_2	3.1	4	71	
2_13_3	5.6	11	93	17.7
2_14_1	1.0	1	70	
2_14_2	2.9	2	71	
2_14_3	5.9	11	95	22.9
2_15_1	0.5	1	66	
2_15_2	2.5	1	70	
2_15_3	5.3	10	98	13.2
2_16_1	0.6	0	73	
2_16_2	2.5	1	68	
2_16_3	5.0	9	88	12.0
2_17_1	2.0	0	62	
2_17_2	2.8	3	65	
2_17_3	6.1	11	102	17.1
2_18_1	2.1	0	70	
2_18_2	3.3	5	70	
2_18_3	6.0	12	106	17.3
2_19_1	1.0	1	71	
2_19_2	2.5	1	73	
2_19_3	5.3	10	101	13.9
2_20_1	0.7	1	67	
2_20_2	1.0	1	65	
2_20_3	4.2	7	81	10.5
1_9_1	1.7	0	71	
1_9_2	3.2	4	76	
1_9_3	6.3	13	107	19.1
3_9_1	0.5	1	67	
3_9_2	3.5	6	73	
3_9_3	5.6	11	87	14.2
4_9_1	0.5	1	68	
4_9_2	3.2	5	72	
4_9_3	5.5	11	87	15.2
5_9_1	0.5	1	70	
5_9_2	3.0	4	69	
5_9_3	5.5	11	84	13.2

Table B-4. Continued.

Observation column_row_depth	Saturated Paste Extract EC dS m^{-1}	SAR	Percent Moisture	Estimated EC* of soil solution at field moisture level dS m^{-1}
6_9_1	0.5	1	67	
6_9_2	1.2	9	80	
6_9_3	5.5	11	93	17.9
7_9_1	0.5	1	67	
7_9_2	2.0	8	81	
7_9_3	5.7	11	85	16.1
8_9_1	1.0	1	66	
8_9_2	1.5	8	70	
8_9_3	5.5	11	86	13.8
9_9_1	0.5	1	66	
9_9_2	1.0	4	73	
9_9_3	5.0	9	80	12.6
10_9_1	2.2	0	66	
10_9_2	2.4	1	57	
10_9_3	4.6	8	80	9.9
Minimum	0.5	0	54	9.9
Maximum	6.3	13	107	36.6
Mean	3.0	5	75	15.9
Standard Deviation	1.9	4	12	5.6

*Estimated EC of soil solution at field capacity moisture content is calculated by Eq. [17] where 2.2 dS m^{-1} is the maximum EC contributed by gypsum content.

Estimated EC = (EC of saturated paste extract – 2.2) X (saturated paste moisture content/oven dried percent moisture) + 2.2 [17]

Table B-5. Gypsum content and anion concentration in the saturated paste extract of soil cores taken in July.

	Saturated Paste Extract				
OBSERVATION	HCO_3	Cl	SO_4	Sum Anions	Percent
column_row_depth	----------mmol (-) L^{-1}----------				Gypsum
2_1_1	1.6	0.7	8.5	10.8	0.0
2_1_2	1.2	0.2	30.7	32.1	16.4
2_1_3	1.1	2.0	39.8	42.9	8.9
2_2_1	2.8	0.5	0.5	3.8	0.0
2_2_2	1.5	0.0	2.8	4.4	0.0
2_2_3	0.4	3.8	41.1	45.3	6.8
2_3_1	1.8	0.3	2.2	4.2	0.0
2_3_2	0.7	1.4	29.4	31.5	7.6
2_3_3	0.9	8.5	42.6	52.0	3.4
2_4_1	2.1	0.6	9.5	12.2	0.0
2_4_2	0.9	1.8	29.4	32.1	5.3
2_4_3	0.8	8.2	41.0	50.0	9.1
2_5_1	1.2	0.2	14.1	15.4	0.1
2_5_2	0.6	0.0	19.3	19.8	4.0
2_5_3	1.3	4.7	46.3	52.3	18.6
2_6_1	1.1	0.2	20.6	21.9	0.2
2_6_2	0.9	0.4	21.6	22.9	1.4
2_6_3	0.6	5.8	37.8	44.2	14.2
2_7_1	0.9	0.1	18.6	19.6	26.6
2_7_2	1.0	0.1	19.0	20.1	29.0
2_7_3	1.0	4.9	37.8	43.6	7.9
2_8_1	1.2	0.1	5.6	6.9	0.0
2_8_2	0.6	1.7	23.6	25.9	14.8
2_8_3	0.5	7.0	55.6	63.1	2.9
2_9_1	2.1	0.1	0.8	2.9	0.0
2_9_2	1.2	0.6	29.4	31.2	9.0
2_9_3	0.4	6.8	41.0	48.2	1.8
2_10_1	1.5	0.0	1.0	2.5	0.0
2_10_2	0.9	0.2	32.0	33.1	6.9
2_10_3	0.8	5.2	17.1	23.1	4.9
2_11_1	2.0	0.6	0.3	3.0	0.0
2_11_2	1.0	0.3	10.4	11.7	5.6
2_11_3	0.4	3.1	48.3	51.8	3.8
2_12_1	1.6	0.5	17.1	19.2	0.4
2_12_2	0.5	0.2	22.0	22.7	18.1
2_12_3	0.8	3.3	38.1	42.2	17.1
2_13_1	2.1	0.3	1.0	3.4	0.0

Table B-5. Continued.

OBSERVATION column_row_depth	Saturated Paste Extract HCO_3	Cl	SO_4	Sum Anions	Percent Gypsum
	----------mmol (-) L^{-1}----------				
2_13_2	1.6	0.5	31.5	33.5	0.0
2_13_3	0.6	4.2	51.6	56.4	2.4
2_14_1	2.3	0.0	6.3	8.6	0.4
2_14_2	1.0	0.0	26.1	26.8	5.6
2_14_3	0.4	5.0	34.8	40.1	2.5
2_15_1	1.3	0.0	1.4	2.6	0.0
2_15_2	0.8	0.0	27.4	28.2	5.4
2_15_3	0.5	2.9	39.8	43.2	0.3
2_16_1	2.8	0.0	0.7	3.5	0.0
2_16_2	0.9	0.0	26.1	27.0	9.3
2_16_3	0.6	2.5	45.0	48.0	3.6
2_17_1	1.1	0.0	28.6	29.5	20.0
2_17_2	0.9	0.3	31.5	32.6	22.1
2_17_3	0.2	6.0	51.6	57.9	0.7
2_18_1	0.6	0.0	26.5	26.6	2.3
2_18_2	1.5	0.2	30.1	31.8	13.6
2_18_3	0.1	5.4	51.6	57.1	0.6
2_19_1	2.3	0.3	5.1	7.6	0.0
2_19_2	1.3	0.0	23.4	24.5	9.9
2_19_3	0.7	2.0	44.9	47.5	0.5
2_20_1	1.7	1.1	2.5	5.3	0.0
2_20_2	1.8	0.0	5.9	7.7	0.0
2_20_3	0.4	1.6	28.8	30.7	2.6
1_9_1	3.2	0.2	13.6	17.0	0.0
1_9_2	1.2	0.6	39.2	41.0	12.8
1_9_3	1.2	8.0	56.0	65.2	0.0
3_9_1	2.0	0.2	1.0	3.1	0.0
3_9_2	1.0	1.3	38.0	40.3	1.2
3_9_3	0.4	7.4	47.0	54.8	5.8
4_9_1	2.3	0.2	0.7	3.3	0.0
4_9_2	1.0	0.6	29.6	31.2	3.5
4_9_3	0.5	6.6	47.0	54.1	5.3
5_9_1	2.4	0.2	0.5	3.1	0.0
5_9_2	1.2	1.4	24.2	26.8	1.0
5_9_3	0.4	8.8	44.0	53.2	6.2
6_9_1	2.7	0.7	0.9	4.3	0.0
6_9_2	1.3	3.0	9.4	13.7	0.0

Table B-5. Continued.

OBSERVATION column_row_depth	Saturated Paste Extract HCO_3	Cl	SO_4	Sum Anions	Percent Gypsum
	----------mmol (-) L^{-1}----------				
6_9_3	0.7	10.5	47.0	58.2	3.3
7_9_1	1.9	0.0	1.1	2.9	0.0
7_9_2	1.3	2.7	17.2	21.2	0.0
7_9_3	0.0	12.0	44.0	55.9	4.8
8_9_1	2.5	0.7	7.0	10.2	0.0
8_9_2	1.6	3.2	8.8	13.6	0.0
8_9_3	0.2	0.0	50.0	41.7	3.9
9_9_1	2.3	0.3	5.3	7.9	0.0
9_9_2	1.1	0.9	6.0	8.0	0.0
9_9_3	0.4	7.6	27.2	35.2	13.7
10_9_1	2.2	0.0	24.4	26.5	9.4
10_9_2	0.6	0.5	30.4	31.5	29.2
10_9_3	0.7	3.8	41.6	46.1	17.0
Minimum	0.0	0.0	0.3	2.5	0.0
Maximum	3.2	12.0	56.0	65.2	29.2
Mean	1.2	2.1	24.8	28.1	5.3
Standard Deviation	0.7	3.2	17.0	18.5	7.1

VITA

Name: Miranda L. Fox

Education:

Kansas State University, B.S.: Agronomy

Permanent Mailing Address:

3715 E. 13th St., Hays, KS 67601, U.S.A